HBM4EU science and policy for a healthy future

HORIZON2020 Programme
Contract No. 733032 HBM4EU

First report on the state of development of new biomarkers of effect

Deliverable Report

AD14.4

WP14 - Biomarkers of Effect

Deadline: November 2018

Upload by Coordinator: 10 January 2019

Entity	Name of person responsible	Short name institution	Date [Received]
Coordinator	Marike Kolossa-Gehring	UBA	08/01/2019
Grant Signatory	Argelia Castaño	ISCIII	08/01/2019

Entity	Name of person responsible	Short name institution	Date [Approved]
Pillar Leader	Robert Barouki	INSERM	22/11/2018
Work Package Leader	Nicolás Olea	UGR	20/11/2018
Task leader	Nicolás Olea	UGR	20/11/2018

Responsible author	Mariana F. Fernández Vicente Mustieles Andrea Rodríguez Nicolás Olea	E-mail	marieta@ugr.es vmustieles@ugr.es andrearc@ugr.es nolea@ugr.es
Short name of institution	UGR	Phone	
Co-authors	Arthur David (INSERM), Shereen Cynthia (INSERM), Ludek Bláha (MU), Eva Cecilie Bonefeld-Jorgensen (AU), Anne Marie Vinggaard (DTU), Hanna Johansson (DTU), Jean-Philippe Antignac (INRA), Annelaure Damont (CEA).		

Table of contents

Authors and acknowledgements

Lead authors

Vicente Mustieles (UGR)

Andrea Rodríguez (UGR)

Mariana Fernández (UGR)

Nicolás Olea (UGR)

Contributors

Arthur David (INSERM), Shereen Cynthia (INSERM), Ludek Bláha (MU), Anne Marie Vinggaard (DTU), Hanna Johansson (DTU), Eva Cecilie Bonefeld-Jorgensen (AU), Jean-Philippe Antignac (INRA), Annelaure Damont (CEA).

1 Abstract

Background: The European population is exposed to complex mixtures of chemicals at low doses, representing a challenge for both scientific community and policy agencies.

Objective: The main objective of this AD14.4 was to complement the information presented in D14.4, providing additional data on relevant biomarkers of exposure and effect.

Methods: The following biomarkers were used: i) exposure levels of two prioritised environmental chemical families: metals and PFAS in homogenates of placenta samples; ii) hormonal profile of placental homogenates; iii) anti-androgenic activity of placenta extracts (alpha-fractions) using an AR-reporter gene assay; iii) urinary 8-OHdG concentrations, a marker of DNA damage; iv) untargeted metabolomic analysis of placental homogenates; and v) selected epigenetic markers in placental homogenates.

Results: Biomarkers of exposure for PFAS and metals were successfully conducted. Placental extracts (alpha fractions), containing mixtures of persistent and lipophilic chemicals, showed significant anti-androgenic activity. The hormonal profile from placental tissue was successfully quantified, as well as some epigenetic markers such as Histone H2AX phosphorylation (Gamma-H2AX), trimethylation of histone 3 at lysine (H3K4me) and DNA methylation of BDNF, in addition to untargeted metabolomic analysis. Finally, 8OHdG levels were assessed in urine samples coupled to the placentas from the same women.

Conclusions: This collaborative work has shown that chemical mixtures isolated from human samples can be assessed, and its biological activity quantified using different biomarkers cell-based tools. Placenta tissue could be used as a relevant biological matrix to assess both exposure and effect biomarkers. Moreover, we hereby demonstrate that the placenta can be used to explore the implementation of novel effect biomarkers in Human Biomonitoring programs, due to the volume and availability of this biological sample.

Future Steps: i) To investigate the relationship between exposure and effect biomarkers tested in placenta samples (included in D14.4 and AD14.4); ii) To assess the implementation of the most appropriated biomarkers of effect and combined effect in other biological matrices more frequently recruited in HBM programs, such as blood and urine; iii) To explore the concentration to specific chemical families, such as PFAS and metabolites, in placenta and serum samples, in order to assess its combined effects on different effect biomarkers such as some *in vitro* cell bioassays.

2 Introduction

Background

Low levels of a wide range of environmental pollutants are present all around the world, and the European population is under the influence of this exposure (Kortenkamp, 2014). The resulting mixture includes myriads of chemical species such as polycyclic aromatic hydrocarbons, polychlorinated dioxins, multiple pesticide residues, persistent organic pollutants, heavy metals, phthalates, bisphenols, polybrominated and poly/per-fluorinated compounds together with their metabolites. Therefore, these exposure biomarkers can be found in human matrices (e.g. urine, blood, serum, nails, hair and placenta) and their characterisation in Human Biomonitoring (HBM) programs in combination with effect biomarkers is crucial for risk assessment policies (DeCaprio, 1997; Silbergeld and Davis, 1994). Within this range of pollutants, Perfluoroalkyl acids (PFAS) and some heavy metals are of high concern due to their persistent behaviour in both environment and human body (Fu et al., 2016; Lindstrom et al., 2011). Either metals or PFAS have ubiquitous presence in aquatic environments (Blake et al., 2018; Rehman et al., 2018), therefore, their exposure through drinking water is an actual and on-going community-based concern. However other sources of exposure, including air, diet, and occupational exposure have been taken into account (Esposito et al., 2018). PFAS own no-common properties including thermal stability, resistance to stains and repellence to oil and water (ATSDR, 2009) and their exposure has been associated with several adverse health effect in humans, such as alterations in thyroid function (Ballesteros et al., 2017), kidney function (Shankar et al., 2011; Watkins et al., 2013), and metabolism (Fisher et al., 2013; Lin et al., 2009). On the other hand, heavy metals are able to disrupt metabolic functions into the human body by their accumulation in some vital organs including brain, heart, liver and kidney thus altering their biological functionality (Rehman et al., 2018).

Results obtained from D14.4

The aim of D14.4 ‘Proof of concept’ was to assess a set of biomarkers of combined effect on the same human samples: human placenta. These types of biomarkers are able to estimate how different chemicals act in an additive, synergetic and/or antagonistic way to exert a specific biological activity. Therefore, WP14 partners applied a total of 6 experimental bioassays-biomarkers of combined effect on these samples with interesting implications for HBM. Previous works from UGR and other teams have shown that it is possible to obtain a chemical fraction from human samples (placenta, serum, etc.) in which the most persistent and lipophilic contaminants are found, without the presence of endogenous hormones (Arrebola et al., 2015; Bjerregaard-Olesen et al., 2016; Bonefeld-Jorgensen et al., 2011; Fernandez et al., 2007; Pastor-Barriuso et al., 2016; Vilahur et al., 2014, 2013). Based on this evidence, the first step was to perform this fractionation on the placentas and send the extracts to some partners. Briefly, placenta homogenates are dissolved in hexane and eluted in a glass column filled with Alumine. The eluate obtained is concentrated and injected into a high-pressure liquid chromatography (HPLC) . The HPLC method allows to separate endogenous hormones (β fraction, eluted from 13 to 30 HPLC min) from more lipophilic environmental chemicals (α fraction, eluted from 0 to 11 HPLC min) (mostly bioaccumulated organohalogenated compounds). The **alpha fraction** would be tested in specifics bioassays to assess its biological activity (see D14.4 for extended information) (Figure 1).

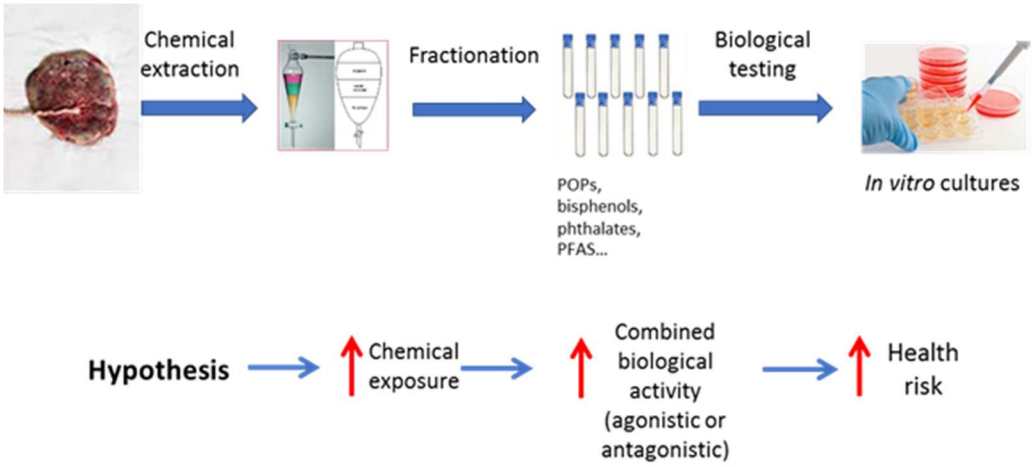

Figure 1: Ex-vivo cell-based assays for assessing the combined biological effect of chemical mixtures extracted from human placentas

An additional HPLC fractionation protocol also allows identifying both individual and several families of man-made chemicals in the 30 1 min possible HPLC poopled fractions (Arrebola et al., 2015) (Figure 2).

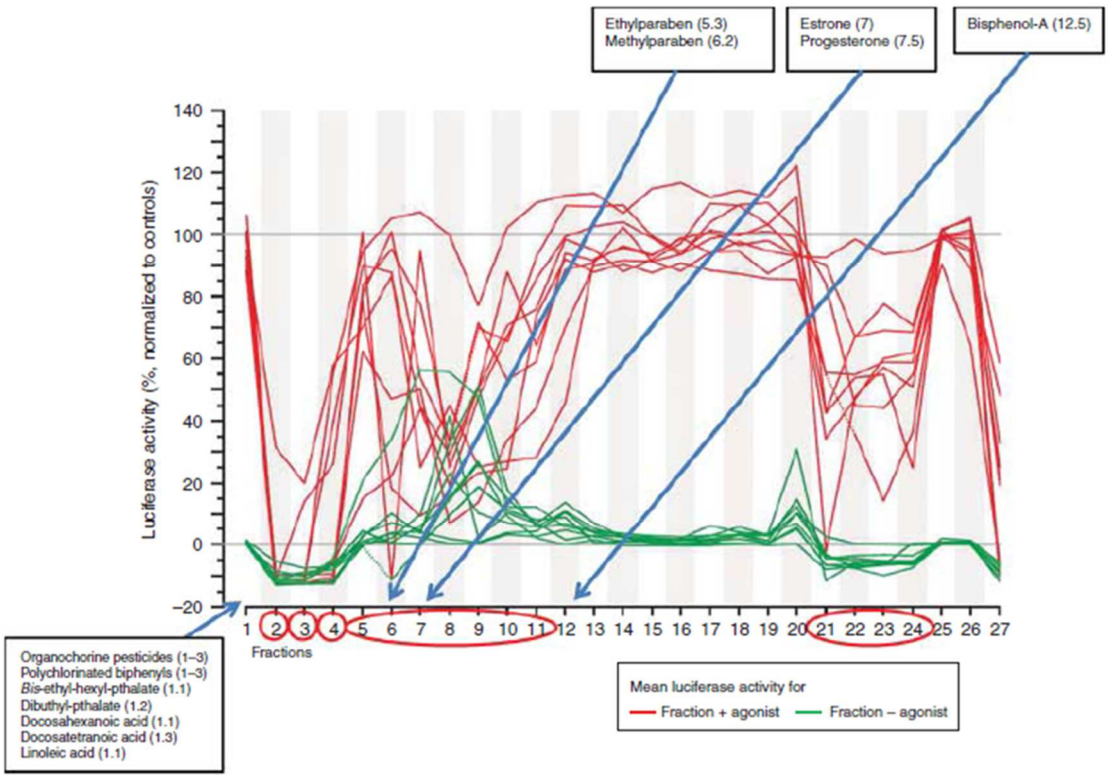

Figure 2: It is also possible to isolate (anti-)androgenic activity in 27 1-min HPLC fractions of placenta samples as well as to assess the retention times (min) of specific spiked chemicals (Arrebola et al., 2015).

The aim of D14.4 'Proof of concept' was to conduct bioassays together with specific biomarkers of combined effect, such as: i) Estrogenic activity was found for all placental alpha-fractions, ii) in the Xenopus Laevis assay, alpha-fractions tended to produce an antagonism of thyroid activity; iii) few alpha-fractions indicated alterations in the Aryl hydrocarbon receptor (AhR) assay. In addition, two markers of oxidative stress and biological ageing were successfully assessed in placental pieces: a) Telomere length, a known marker of biological ageing and b) levels of 8-OHdG, a marker of DNA damage, as well as an indirect marker of oxidative damage. Since additional information has been generated, AD14.4 contains complementary data on both exposure and effect biomarkers to further understand the results initiated in D14.4, and plan the implementation of novel effect biomarkers of interest for HBM4EU aligned studies, as well as using other matrices such as urine and blood/serum, more frequently used in HBM studies.

Assessing the combined effect of chemical mixtures: Bioassays complementary to D14.4

Thus, this Additional Deliverable 14.4 (AD14.4) will provide more information regarding previous bioassays. INRA has measured PFAS levels in placental homogenates (Kadar et al., 2011; Yamada et al., 2014) and INSERM has measured all heavy metals present in placental samples. Meanwhile, the AR-reported gene-assay was repeated in order to better assess the anti-androgen activity of placental samples and a specific assay for cytotoxicity was also conducted. INRA also developed the hormonal profile of placental samples (using whole placenta homogenised). INSERM conducted untargeted metabolomics analyses and epigenetics biomarkers previously identified in the literature searches (D14.2 and D14.3), such as DNA methylation of BDNF. Finally, to see if 8-OHdG is a feasible effect biomarker for HBM4EU, MU developed a LC-MS methodology to measure this metabolite in 85 urine samples, corresponding to the same women that donated the 25 placentas (each woman gave a total of 3 urine samples at the three pregnancy trimesters, in addition to the placenta and a urine sample at delivery).

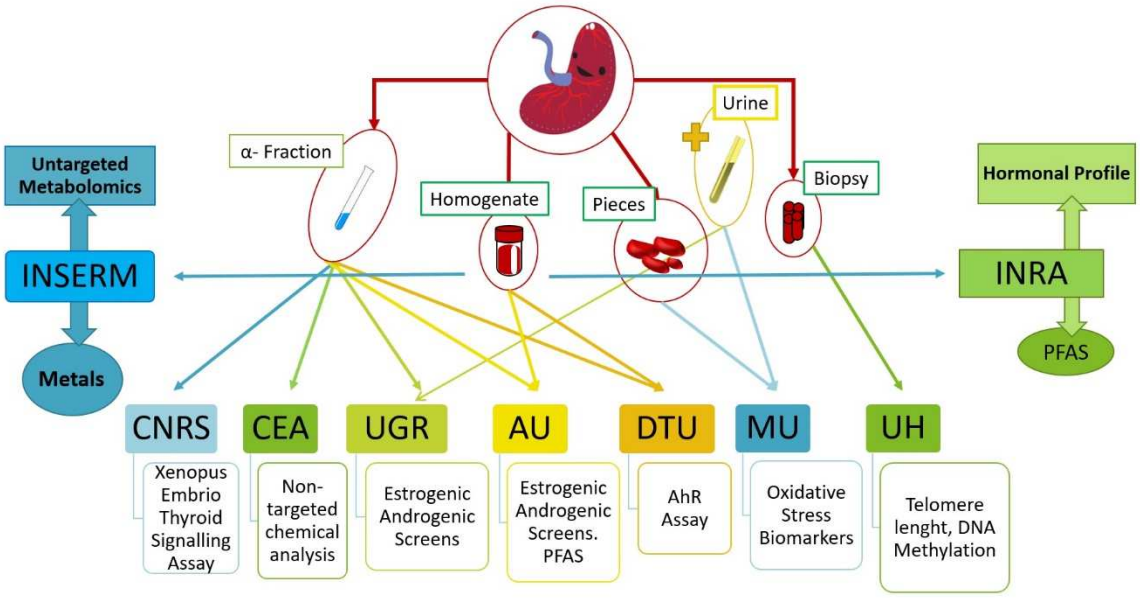

Scheme 1: Experimental flow showing all bioassays and biomarkers assessed with whole placenta tissue, placenta alpha fractions and urine, as well as WP14 partners involved.

Aim of the deliverable

The main objective of this AD14.4 was to conduct different bioassays and/or possible biomarkers of combined effect, together with exposure biomarkers, using the same placentas employed in D14.4, but also studying maternal prenatal urine samples coupled to these same placentas, in order to: i) further characterise the exposure and effect profile of the samples under study; ii) improve some of the previous bioassays tested (AR-screen, this time conducted by DTU); iii) complement and further understand possible exposure-effect relationships regarding chemical mixtures; iv) implement novel effect biomarkers that could be of interest for HBM4EU aligned studies (DNA methylation of BDNF, untargeted metabolomics, etc.).

3 Planning and Distribution of Tasks

Table 1: Tasks conducted by each team

Summary of Bioassays			
PARTNER	**Responsible**	**Biological material shipped**	**Bioassays/Biomarkers**
UGR	Nicolás Olea	UGR designed, planned and coordinated all the work conducted within D14.4 and AD14.4. Additionally, UGR provided all the biological materials analysed, obtained the tested alpha-fractions from placentas, and conducted all the shipments to each of the partners listed below.	
INRA	Jean-Philippe Antignac	25 placental homogenates (≈20g)	Exposure biomarker: Identification of PFAS metabolites in placenta homogenates
INRA	Jean-Philippe Antignac	25 placental homogenates (≈20g)	Effect biomarkers: Hormonal profile in placenta homogenates
INSERM	Arthur David	25 placental homogenates (≈20g)	Exposure biomarkers: Metals profile in placenta homogenates
INSERMS-INRA-CEA	Arthur David; Jean P. Antignac; Annelaure Damont	25 placental homogenates (≈20g)	Effect biomarkers: Untargeted metabolomics and epigenetic markers.
DTU	Anne Marie Vinggaard	25 α-Fraction 25 Placental Homogenate (≈20g)	Biomarker of combined effect: Anti-androgenic activity of placental alpha fractions tested in an AR reporter gene assay.
MU	Ludek Blaha	85 urine samples paired to the 25 placentas studied	MU has fine-tuned a LC-MS methodology for the measurement of 8-OHdG in urine.
AU	Eva Cecilie Bonefeld Jorgensen	25 Placental homogenates (≈20g)	New methodology to isolate mixtures of PFAS metabolites in placenta and serum (Future Steps) that can be tested for different biological activities.

4 Methods

4.1 PFAS measurements in placental homogenates (INRA)

Half of the placentas without deciduas basalis and chorionic plate, collected at the time of delivery and frozen immediately at −80°C, are almost defrosted and mechanically homogenised and aliquoted into 25 g placenta samples. The analytical method used to determine the concentrations of the PFAS related markers in placenta homogenates was described elsewhere (Kadar et al., 2011; Yamada et al., 2014). The 14 targeted compounds included perfluorooctane sulfonate (PFOS), perfluorobutane sulfonate (PFBS), perfluorohexane sulfonate (PFHxS), perfluoroheptane sulfonate (PFHpS), perfluoro-1-decanesulfonate (PFDS), perfluorooctanoic acid (PFOA), perfluorobutanoic acid (PFBA), perfluoropentanoic acid (PFPA) perfluorohexanoic acid (PFHxA), perfluoroheptanoic acid (PFHpA), perfluorononanoic acid (PFNA), perfluorodecanoic acid (PFDA), perfluoroundecanoic acid (PFUnA), and perfluorododecanoic acid (PFDoA).

Briefly, samples were freeze-dried and extracted with methanol. After evaporation, the resulting crude extracts were purified onto two consecutive solid-phase extraction (SPE) columns (copolymeric reversed phase and charcoal). Purified extracts were then analysed by liquid chromatography coupled to tandem mass spectrometry (LC–MS/MS) using electrospray ionisation in the negative ion mode and at least two diagnostic signals (MRM transitions) per analyte. Quantification was performed according to the isotope dilution principle using 13C-labelled internal standards (13C4-PFOA, 13C4-PFOS, 13C4-PFBA, 13C5-PFHxA, 13C4-PFHpA, 13C5-PFNA, 13C2-PFDA, 13C7-PFUnA, 13C2-PFDoA, and 18O2-PFHxS.

4.2 Metal profile in placental homogenates (INSERM)

For each placenta sample, 0.25 g of freeze-dried placenta is mixed with 5 ml of nitric acid and 1 ml of hydrogen peroxide in 70 ml bomb of the Ethos1 microwave (Milestone).

After digestion in microwave, the mineralised samples are diluted in 100 ml of ultrapure water and 2 ml of hydrochloric acid, and analysed by ICP-MSMS 8800 (Agilent technologies). The sample is nebulised by a microflow system.

For quantitative analysis, the mass spectrometer is used in helium, hydrogen or oxygen mode, depending on the elements and performed for 15 elements: Be, V, Mn, Cu, Zn, Se, Ag, Cd, Cs, Ba, Tl, Pb, Bi, U, Hg. Each sample is analysed twice and carried out in one batch with 8 analytical blanks and 3 reference blood samples for mineralisation control (Utack, INSPQ). Six internal standards are added in each sample and calibration point.

For qualitative analysis, the mass spectrometer is used in scan mode (7 to 238 uma) with helium mode and performed for 22 elements: Li, Na, Mg, Al, K, Ca, Ti, Cr, Fe, Co, Ni, As, Sr, Mo, Ru, Sb, La, Ce, Nd, Gd, Lu and Th.

Table 2: ICP-MSMS Acquisition Parameter

Elements	Isotopes used	Internal standard	Curve	Gas mode
Li	6/7	Ge^{72}	linear	No gas
Be	9	Sc^{45}	linear	No gas
Na	23	Sc^{45}	linear	He
Mg	24/26	Sc^{45}	linear	He
Al	27	Sc^{45}	linear	No gas, He, O_2
K	39	Sc^{45}	linear	He
Ca	43/44	Sc^{45}	linear	-
Ti	47/49	Sc^{45}	linear	He
V	51	Ge^{72}	linear	He
Cr	52/53	Ge^{72}	linear	He
Fe	54/56/57	Sc^{45}	linear	He
Mn	55	Ge^{72}	linear	He, O_2
Co	59	Ge^{72}	linear	He
Ni	60/62	Ge^{72}	linear	He
Cu	63/65	Ge^{72}	linear	He
Zn	66/67/68	Ge^{72}	linear	He
As	75	Ge^{72}	linear	He, O_2
Se	78/80	Se^{77}	quadratic	H_2 ,O_2
Sr	86/88	Rh^{103}	linear	No gas
Mo	95/97	Rh^{103}	linear	No gas
Ru	99/101/102	Rh^{103}	linear	No gas
Ag	107/109	Rh^{103}	linear	No gas
Cd	114/111	Rh^{103}	linear	No gas/He
Sn	118/120	Rh^{103}	linear	No gas
Sb	121/123	Rh^{103}	linear	No gas
Cs	133	Re^{185}	linear	No gas
Ba	133/137	Re^{185}	linear	No gas
La	139	Re^{185}	linear	No gas
Ce	140	Re^{185}	linear	No gas
Nd	143/146	Re^{185}	linear	No gas
Gd	157	Re^{185}	linear	No gas
Lu	175	Re^{185}	linear	No gas
Hg	199/200/201/202	Ir^{193}	linear	No gas

Elements	Isotopes used	Internal standard	Curve	Gas mode
Tl	203/205	Ir ^{193}	linear	No gas
Pb	208/206/207	Ir ^{193}	linear	No gas
Bi	209	Ir ^{193}	linear	No gas
Th	232	Ir ^{193}	linear	No gas
U	238	Ir ^{193}	linear	No gas

4.3 Hormonal profile in whole placental homogenates (INRA)

The analytical method used to determine the concentrations of the steroid related markers was described elsewhere (Courant et al., 2010).

The 33 targeted compounds included Pregnenolone, 17aOH- pregnenolone, DHEA, 5-androstene-3a,17b-diol, 5-androstene-3b,17a-diol, 5-androstene-3b,17b-diol, Progesterone, 17aOH-progesterone, Androstendione, 17β-testosterone, 17α-testosterone, 5α-pregnane-3,20-dione_(Dihydroprogesterone), 5α-pregnane-17α-ol-3,20-dione_(17αOH-dihydroprogesterone), 5α-Androstanedione, 5β-Androstanedione, 5α-dihydrotestosterone_(5α-DHT), 5α-pregnane-3α-ol-20-one_(Allopregnanolone), 5α-pregnane-3α,17-diol-20-one_(17αOH-Allopregnanolone), Androsterone, Epiandrosterone, Etiocholanolone, 5α-Androstane-3α,17α-diol, 5α-Androstane-3α,17β-diol, 5α-Androstane-3β,17α-diol, 5α-Androstane-3β,17β-diol, 5β-Androstane-3α,17α-diol, 5β-Androstane-3α,17β-diol, 5β-Androstane-3β,17α-diol, 5β-Androstane-3β,17β-diol, 17α-estradiol, 17β-estradiol, and Estrone. Briefly, tissue samples were ground in the presence of methanol/water 80:20 (v:v). The resulting mash was transferred in glass tubes, and the methanol layer was evaporated under N_2 stream. Then, an enzymatic deconjugation was performed on a first aliquote of each sample for giving access to the concentration of the total forms (free+deconjugated) of the considered markers. The deconjugation of both glucuronide and sulphate forms was operated overnight at 37°C using a preparation of β-glucuronidase from *Patella vulgata* and Arylsulfatase from *Helix pomatia*. No enzymatic hydrolysis was performed on a second aliquote of each sample to have access to the concentration of free forms only. The target steroids were then extracted twice with methylterbutylether (MTBE), and purified onto a ChromP SPE cartridge. A liquid/liquid partitioning with pentane was further used to separate androgens/progestogens from estrogens, and the two resulting fractions were finally submitted to a further purification through silica (SiOH) solid-phase extraction cartridges. The measurement was performed by gas-chromatography coupled to tandem mass spectrometry (GC-MS/MS), after electron impact (EI). Two diagnostic signals (SRM transitions) were monitored for each target analyte, providing unambiguous identification. Stable isotope surrogates (2H-labelled compounds) were included for individual recovery correction and quantification according to the isotope dilution method, including 17β-testosterone-d3, methyltestosterone-d3, androstendione-d3, 5α-dihydrotestosterone-d3, etiocholanolone-d5, 5α-androstane-3α,17β-diol-d3, 5α-androstane-3β,17β-diol-d3, and 17β-estradiol-d3.

4.4 Untargeted metabolomics (INSERM-INRA-CEA)

This protocol was based on a Bligh & Dyer extraction commonly used in the metabolomics and lipidomic communities. This methodological biphasic extraction appears as an efficient approach to extract and split each analysed sample in two main fractions, namely a polar and non-polar respectively. INRA performed all placenta extractions according to the protocol described below and then sent aliquots of both polar and non-polar fractions to INSERM and CEA.

Briefly, 100 mg of placenta was weighed in Precellys® tube. 150 µL of water, 250 µL of methanol containing a mixture of QA/QC internal standards for both positive and negative modes and 400 µL of chloroform were added, with 30 seconds of vortex after each addition. Samples were homogenised twice during 30 seconds at 6 000 rpm with a pause of 45 seconds between each. After 15 minutes of centrifugation at 4°C and 13 000 g, the polar (water/methanol) phase was isolated from the non-polar (chloroform) phase. Each partner laboratory received 50 µL of each extract. They added their own external standards and reconstituted the samples in the solvent of injection according to their own analytical procedures.

INRA performed a non-targeted profiling of placental extracts using reverse phase (C_{18}) liquid chromatography coupled to high resolution mass spectrometry (LC-HRMS) on a Q-Exactive (Orbitrap) instrument after electrospray ionisation. Polar and non-polar fractions were analysed in negative ionisation mode. INSERM performed the untargeted profiling of both polar and non-polar fractions using a reverse phase (Acquity UHPLC HSS-T3) on a UHPLC-ESI-Q-TOF (X500R, Sciex) in positive and negative MS modes.

INSERM performed preliminary treatment of datasets as a first step to identify potential groups of placenta. First, datasets were deisotoped, the mass spectral peaks deconvolved, aligned, and the peak areas integrated and normalised to the total spectral area. The datasets, comprising many thousands of retention time x m/z variables were Pareto scaled and log prior to principal components analysis (PCA) to examine potential differences between group samples and to detect sample outliers. Orthogonal partial least-squares discriminant analyses (OPLS-DA) were used to investigate metabolite differences between identified placenta groups (see **Figure 12** in the result section, as example). Compounds discriminating between exposure groups were detected using t-test. The commercial software MarkerView was used to perform this data treatment but open source software such as MZmine 2 could be used in the future to improve pre-processing of the datasets and further confirmation of the statistical analyses. Preliminary identification of compounds was done from the accurate mass, isotopic fit, fragmentation data obtained from high energy collisional-induced dissociation and from comparison with an in-house library. Databases such as PubChem, METLIN or my Compound Identification were used to search the structural identity of the metabolites.

4.5 Anti-androgenic activity of placenta alpha fractions (DTU)

The AR reported gene assay is based on the stably transfected AR-EcoScreen^{TM} cell line, which are derived from a Chinese hamster ovary cell line (CHO-K1). The cell line has three inserted constructs. These include a human AR expression construct encoding the full-length human gene, a firefly luciferase reporter construct followed by a minimal heat shock protein promoter and a Renilla luciferase reporter construct under the SV40 promoter. This Renilla luciferase reporter is constitutively and non-inducible expressed to distinguish pure antagonism from a decrease in luciferase activity due to cytotoxicity. Binding of a ligand to the AR will increase (being an agonist) or decrease (being an antagonist) the cellular expression of the luciferase reporter gene, resulting

in a change in luminescence, which can then be quantitatively measured. This makes it possible to evaluate whether a test compound or sample acts as a disruptor of androgen signaling. The Dual-Glo® Luciferase Assay System Protocol from Promega (Madison, Wisconsin, USA) was used to quantify the stable luminescent signal from the two reporter genes. The kit consist of Dual-Glo® Luciferase Reagent which induces cell lysis and acts as a substrate for firefly luciferase and Dual-Glo® Stop & Glo® Reagent which quenches the luminescence from the firefly reaction and provides the substrate for Renilla luciferase, thus the Dual-Glo® Stop & Glo® Reagent facilitates the measurement of any potential cytotoxicity.

4.5.1.1 Cell culture

The AR-EcoScreen™ cell line (JCRB1328) were purchased from the Japanese Collection of Research Bioresources Cell Bank (JCRB Cell Bank) and cultured as a monolayer in CellBIND® Surface cell culture flasks (Corning® Inc., Corning, New York, USA) in growth medium consisting of Gibco® Dulbecco's Modified Eagle Medium F-12 Nutrient Mixture with L-glutamine and HEPES and without phenol red (DMEM/F-12) (Invitrogen™, Life Technologies™, Carlsbad, California, USA) supplemented with 5 % Fetal Bovine Serum (FBS) (Invitrogen™, Life Technologies™, Carlsbad, California, USA), 1 % Penicillin-Streptomycin (Invitrogen™, Life Technologies™, Carlsbad, California, USA), 200µg/ml Zeocin™ Selection Reagent (Invitrogen™, Life Technologies™, Carlsbad, California, USA), and 100µg/ml Hygromycin B (Invitrogen™, Life Technologies™, Carlsbad, California, USA). Cells were passaged when reaching 90 % confluence by rinsing the cell monolayer once with pre-warmed (37^{O}C) phosphate buffer saline (PBS) (VWR, Radnor, Pennsylvania, USA) following addition of 0.05 % Trypsin-EDTA solution (Sigma-Aldrich®, St. Louis, Missouri, USA) and incubation at room temperature for 5 minutes. When the cell-layer was dispersed, the Trypsin-EDTA solution was deactivated by adding assay medium consisting of DMEM/F-12 medium supplemented with 5 % dextran-coated charcoal stripped FBS (DCC-FBS) (Sigma-Aldrich®, St. Louis, Missouri, USA) and 1 % Penicillin-Streptomycin (Invitrogen™, Life Technologies™, Carlsbad, California, USA) 3x the volume of the applied Trypsin-EDTA solution.

The cells were aspirated, re-suspended and dispersed into CellBIND® Surface cell culture flasks or 96-well plates. The cells were kept in an incubator at 37^{O}C in 5% CO_2 in a humidified atmosphere.

4.5.1.2 Dissolution of placenta samples

The twenty-four placenta alpha fractions extracts, each prepared from 3 g whole homogenised placenta, were aliquoted into four vials of 100 µL each. One vial of 100 µL was evaporated for the AR reporter gene assay solubilised in 250 µL AR assay culture medium (3 mg placenta/µL). Successively, the extracts were left to rest for 30 min after which they were filtered through a 0.22 µm filter.

The placenta extracts were tested in triplicates together with a medium control, which was tested in six replicates per 96-well plate. From the 250 µL solubilised placenta extract, a 600-, 180-, and 60-fold dilution was prepared and tested. These dilutions correspond to 0.005, 0.017 and 0.05 mg placenta/µL (0.5, 1.7 and 5 mg placenta per well).

4.5.1.3 Experimental set-up

Metribolone (R1881, CAS No. 965-93-5, PerkinElmer, Waltham, Massachusetts, USA) was used as the positive control for agonistic activity and tested in eight concentrations ranging from 0.002-2700 nM. Hydroxyflutamide (OHF, CAS No. 52806-53-8, Toronto Research Chemicals, Toronto, Ontario, Canada) was used as the positive control for antagonistic activity and tested in eight concentrations ranging from 31-8000 nM. DMSO was used as vehicle control and was constant at

0.1% across all exposure groups and the vehicle control group. Both vehicle control and positive controls were tested in triplicates.

Cells were seeded in a concentration of 9000 cells/well in white 96-well plates (Corning® Inc., Corning, New York, USA) (100 µL per well) and left to incubate for ~24 h after which cell culture medium was removed and placenta extract or control compounds were added in varying concentrations.

As the assay was run in antagonist mode 0.1 nM R1881 was added to all wells including the medium control. After approximately 20h incubation, 100µl Dual-Glo® Luciferase Reagent was added to each well and the plates were placed at room temperature on a shaking table for approximately 15min. The firefly luminescence was measured using the LUMIstar® Galaxy luminometer (BMG LABTECH, Offenburg, Germany).

4.5.1.4 Cell viability

Cytotoxicity was examined using Dual-Glo® Stop & Glo® Reagent from the Dual-Glo® Luciferase Assay System from Promega (Madison, Wisconsin, USA), as previously mentioned.

After measurement of the firefly luminescence the plates were supplemented with 50µl/well of Dual-Glo® Stop & Glo®. The plates were placed at room temperature on a shaking table for approximately 15 min following measurement of Renilla luminescence using the LUMIstar® Galaxy luminometer (BMG LABTECH, Offenburg, Germany). This was done in order to distinguish a decrease in luciferase activity due to antagonistic activity from cytotoxicity.

Both the AR antagonist assay and the cell viability test in the CHO cell-line were tested in three independent experiments.

4.6 Urinary measurements for 8-OHdG (MU)

Chemicals

Standard 8-hydroxy-2'-deoxyguanosine (8-OHdG, 98 %) and 2-deoxyguanosine monohydrate (2dG, 99-100 %) were obtained from Sigma-Aldrich (Merck); 15N5-8-hydroxy-2′-deoxyguanosine (>95 %) were obtained from Cambridge Isotope Laboratories; MS grade acetonitrile, isopropanol and formic acid (FA, 99%) were purchased from BIOSOLVE BV (Netherlands).

Extraction of urine

The urine samples kept in -80 °C were thawed at room temperature and vortexed. The 10 □L of internal standard ^{15}N5-8-OHdG (^{15}N5-8-hydroxy-2′-deoxyguanosine; 1 □g/mL in 0.1% v/v formic acid) was added to 0.5 mL of each urine samples (or to calibration solutions of 8-hydroxy-2′-deoxyguanosine; 0, 0.5, 5, 50 ng/mL in 0.1% v/v formic acid) using 2 mL plastic vials. Samples were well vortexed, then frozen at -80°C overnight and lyophilized/freeze dried for 24h. Dry urine and calibration samples were re-suspended in 0.5 mL of isopropanol and extracted in ultrasonic bath for 15 min. Insoluble particles were removed by centrifugation (12,000 x g, 10 °C, 10 min), 350 µL of supernatant was evaporated in a glass vials by stream of nitrogen to dryness (approx. 15min), and dissolved in 250 µL of 0.1% v/v formic acid using ultrasonic bath and vortex. Residual particles were removed by micro-spin filters (0.2 µm; cellulose acetate; 10 000 x g, 3 min, 10 °C). Filtrates in glass vials were stored in -80 °C until the analyses by LC-MS/MS – undiluted samples were analysed for 8-OHdG by LC-MS/MS, while the samples diluted 1,000-times using 0.1% of formic acid were used for analyses of creatinine. Simple validation was performed by the extraction

of spiked urine and blank samples using 2 different 8-OH-dG concentrations (5 and 50 ng/mL) and isopropanol as a solvent. Recovery (Table 3) ranged from 98 to 107%.

Table 3: Simple validation of extraction procedure

Sample	Spike of 8-OHdG (ng/mL)	Concentration after extraction (ng/mL)	Recovery (%)
0.1 % formic acid	0.0	0.0	
0.1 % formic acid	5.0	5.3	106.8
0.1 % formic acid	50.0	49.6	99.2
urine	0.0	2.1	
urine	5.0	7.0	97.5
urine	50.0	51.9	99.6

4.5.1 Analyses by LC-MS/MS

Analyses of 8-OHdG were performed with Waters Acquity LC chromatograph (Waters, Manchester, U.K.) consisting of a vacuum degasser, a binary pump, a thermostatted autosampler, and a column compartment. The column used was an Acquity UPLC BEH C18 (1.7 µm) (Waters) 100 x 2.1 mm equipped with a guard pre-column kept at 25°C. Detection was performed on a Xevo TQ-S quadrupole mass spectrometer (Waters Manchester, U.K.) equipped with electrospray ionisation. Analytes after ESI ionisation were detected in positive ion mode using tandem mass spectrometry with multiple reaction monitoring (MRM). Data were processed by MassLynx^{TM} software (Manchester, U.K.).

4.5.2 Analyses of 8-OHdG in urine

The mobile phase consisted of 0.1% formic acid in water (A) and acetonitrile acidified by 0.1% formic acid (B). The binary pump gradient was linear (5% B at 0-1 min, then increases from 5% B at 1 min to 80% B at 5 min and 80% B was kept for 2 min) followed by 4 min column equilibration to the initial conditions (5% B). The flow rate was 0.2 mL/min, and 10 µL of individual sample from the thermostatted autosampler (10°C) was injected for the analyses. The ionisation parameters were as follows: capillary voltage, 2.5kV; the source temperature and the desolvation temperature, 150 and 750 °C, respectively; the cone gas flow, 150 (L/h); the cone voltages, 30 V; the desolvation gas flow, 750 (L/h); and the collision gas flow, 0.15 mL/min. The collision energy was optimised for each analyte (**Table 4**). Retention time was 3.1 min, limit of quantification (S/N>3) was 0.05 ng/mL. Concentration of 8-OHdG were corrected for the content of internal standard and expressed as microgram per liter of urine as well as microgram per gram of creatinine (method for creatinine analysis is below).

Table 4: LOD and MS parameters for 8-OHdG and internal standard

Compound	LOD (ng/mL)	MRM transitions	collision energy (V)
8-OHdG	0.01	284.1 → 168.1	14
		284.1 → 140.1	28
^{15}N5 -8-OHdG		289.1→ 173.1	14
		289.1→ 145.1	28

4.5.3 Analyses of creatinine in urine

The flow rate 0.2 mL/min of 5% of acetonitrile acidified by 0.1% formic acid for 5 min was used and 2 µL of individual diluted sample (from the thermostatted autosampler 10°C) was injected for the analyses. The ionisation parameters were as follows: capillary voltage, 3kV; the source temperature and the desolvation temperature, 150 and 450 °C, respectively; the cone gas flow, 150 (L/h); the cone voltages, 36 V; the desolvation gas flow, 600 (L/h); and the collision gas flow, 0.15 mL/min. The collision energy 10 V for both creatinine transitions 114.2 → 44.1 and 114.2 → 86.0 was used. The retention time was 1.28 min and external calibration (10 - 1500 ng/mL) was used for quantification and concentration was expressed as milligrams of creatinine per liter of urine.

4.6 Epigenetics Biomarkers (INSERM)

4.6.1 Histone H2AX Phosphorylation (Gamma-H2AX)

Histone extraction: Histone proteins were extracted from all the 25 placenta samples by using the histone extraction kit from abcam (ab113476). 100 mg of the placental tissue homogenate from each sample was used for histone extraction. Briefly, tissue was disrupted in a tissue lyser (Qiagen) by adding pre-lysis buffer (1X dilution). The lysate was then centrifuged at 10,000 rpm for 5 min at 4°C. This step helps to remove the lysed cytoplasm and recover the nuclei. The pellets were re-suspended in 3 volumes of lysis buffer which contains 0.5 N HCl, and incubated on ice for 30 min. Histones, being basic, are acid soluble while other proteins gets precipitated out. 0.3 volume of Balance-DTT buffer was added to the supernatant and protein was quantified. Protein concentrations were estimated by using Pierce 660 nm protein assay (ThermoScientific, France).

Western blot: 10 µg of histone protein extract from each sample was loaded on a mini-PROTEAN TGX 4–20% precast gel (Bio-Rad) and transferred to a PVDF membrane (Merck Millipore, ISEQ07850). The samples were loaded in the order as shown in the table below. The membranes were incubated in Ponceau S reagent for a few minutes to stain the protein bands. This served as the loading control. Membranes were incubated with anti-phosphorylated histone H2AX rabbit polyclonal primary antibody (Trevigen 4418-APC-100; 1: 500 dilution) overnight at 4°C. After three washing steps, the membranes were incubated with secondary antibody (Anti-rabbit IgG, horseradish peroxidase-linked; 1:10,000 dilution) for 1 h. The signals were revealed with Chemiluminescent HRP substrate (Merck Milipore). The intensity of the bands was measured using ImageJ software.

Table 5: Internal codes for placental samples

Sample No.	Sample ID	Sample No.	Sample ID	Sample No.	Sample ID
1	7032	10	105086	19	17292
2	100208	11	39897	20	76748
3	27759	12	44224	21	C59180
4	107660	13	122741	22	145644
5	49402	14	C30543	23	54472
6	146266	15	140002T	24	125492
7	146433	16	C135915	25	C12939
8	37716	17	C90851		
9	C151676	18	C44135		

4.6.2 Trimethylation of histone 3 at lysine 4 (H3K4me3)

We used 12 placental samples that exhibited low and high gamma H2AX for the analyses (please see the report on gamma H2AX biomarker) due to the fact that H3K4me3 is involved in DNA transcription and repair. The samples that were present in each cluster are provided in the scheme below.

Table 6: Samples present in each cluster

Clusters	Sample Nos.
Cluster 1	7032, 100208, 27759, 49402, 17292, 76748, 54472
Cluster 4	39897, 122741, 140002T, C90851, C59180, C12939

In this study, we used chromatin immpunoprecipitation (ChIP) technique to study a few selected genes enriched with H3K4me3 mark. ChIP is a powerful technique that helps to evaluate the associations of proteins with specific regions of the DNA. The important steps in this technique are (a) cross-linking DNA and proteins by using paraformaldehyde (b) shearing the DNA-protein complexes into ~500 bp fragments by sonication (c) Selectively immunoprecipitating cross-linked DNA and proteins by using antibody (d) Elution and reverse cross-linking DNA-protein associations followed by deproteinisation, and finally (e) purification and analysis of DNA. The detailed protocol is as follows:

Chromatin immpunoprecipitation (ChIP) using antibody against H3K4me3: ChIP was conducted as previously described (Smagulova et al. 2011), with small modifications. Briefly, placenta homogenates were fixed for 10 min in 1% (wt/vol) formaldehyde for crosslinking. After quenching with glycine, the tissue was homogenised using Tissue Lyzer (Qiagen), filtered through a 40-µm cell strainer, and washed in the following buffer: 0.25% (vol/vol) Triton X-100, 10 mM EDTA, 0.5 mM EGTA, 10 mM Tris pH8. Cells were lysed in 0.6 ml of the lysis buffer (1% (wt/vol) SDS, 10 mM EDTA, and 50 mM TrisCl pH8) with a complete protein-inhibitor cocktail (Roche), and the chromatin was sheared to ~500 bp by sonication. The sample was diluted 6 times in ChIP

buffer (0.01% (wt/vol) SDS, 1.1% (vol/vol) Triton X-100, 1.2 mM EDTA, 16.7 mM TrisHCl, 167 mM NaCl). Chromatin was incubated with H3K4me3 antibody (Merck 07-473: Anti-trimethyl-Histone H3 (Lys4) (rabbit polyclonal) overnight at 4°C with Dynabead beads (10002D, Invitrogen). The beads were washed in the following buffers: 1) 0.1% (wt/vol) SDS, 1% (vol/vol) Triton X-100, 2 mM EDTA, 20 mM TrisHCl, 150 mM NaCl; 2) 0.1% (wt/vol) SDS, 1% (vol/vol) Triton X-100, 2 mM EDTA, 20 mM TrisCl pH8, 500 mM NaCl; 3) 0.25 M LiCl, 1% (vol/vol) Igepal, 1 mM EDTA, 10 mM TrisCl, pH8, 1% (wt/vol) deoxycholic acid; 4) TE (twice). The chromatin was eluted by 1% (wt/vol) SDS, 0.1 M NaHCO3 pH9 at 65°C, and crosslinking was reversed at 65°C for 5 hours. The DNA was deproteinised for 1 hour with proteinase K and purified with a MiniElute Reaction Clean-Up kit (Qiagen). The DNA concentration was measured using Quantifluor dsDNA system, (E2670, Promega). Equal amount of ChIP and input DNA were taken for qPCR.

Primer design and qPCR: For the ChIP primer design, the H3K4me3 data (bed and bigWig files) for human placentas from male and female foetuses were downloaded from the ENCODE database (https://www.encodeproject.org/). With the help of Integrative Genomics Viewer (IGV) software, the exon regions that align with the H3K4me3 peaks (for both males and females) were selected for the genes of interest, and the genomic coordinates of the selected regions were noted. The DNA sequences of the selected genomic coordinates were retrieved from UCSC genomic browser (GRCh38/ hg38 assembly) and the sequences were blasted using NCBI Primer-Blast. The selected primer sequences and their chromosome locations are provided in the scheme below.

qPCR was performed on 12 ChIP and 2 input DNA samples. Briefly, forward and reverse primers for each gene (0.1 µl each) and SYBR Green Supermix (BioRad) were mixed with each ChIP samples (0.05 ng/ µl) and were loaded onto qPCR plates and was run on BioRad CFX 384 Real-time PCR system under normal qPCR thermal cycling conditions. The data was analysed by using the BioRad CFX Manager software.

Table 7: Selected primer sequences and their chromosome locations

Gene	Chromosome	Forward Primer	Reverse primer
ESR1	chr6 (151807953; 151808345)	ACTCAACAGCGTGTCTCCGA	GGGCTCGTTCTCCAGGTAGT
ESR2	chr14 (64337896; 64338558)	CAGTGTGGACGCCTACGAG	GATTTTGTCACCCGCACGTC
PGR	chr11 (101127750; 101128302)	TTATCTTTAGAGCGGGCGGC	GGAGTTCACCCTGTGCCTC
BDNF	chr11 (27700160; 27700460)	TACCTCGGGGTCCACACAAA	CTTTAATGAGACACCCACCGCT
H2AFX	chr11 (119094963; 119095395)	ACGGTGGCGCTGGTCTTC	CCATCCGCAACGACGAGG
AHR	chr7 (17298702; 17299420)	GGAAGCACCCTGGATTTAGGAA	TTAGAATCCTGGCCTGGGTCG
PPARG	chr3 (12288129; 12288846)	TTGTGCTGGCCCTACGC	AAAGCAGCGACTTCGCCTTT
RARA	chr17 (40318231; 40318538)	CGGGTAAAGTTTCAGCCTCCG	GCGTCTGCCCTAACCCG
ESRRA	chr11 (64305842; 64306462)	GCAACTTCCCAAAGGTGTGC	AGCCTGCAGGTCCACTCTTA
ACTB	chr7 (5530084; 5530646)	GCTGGCCGGGCTTACC	CGGCGCCCTATAAAACCCA
GAPDH		GCTCACTGGCATGGCCTTCCGTGT	TGGAGGAGTGGGTGTCGCTGTTGA

4.6.3 DNA methylation of BDNF

We analysed BDNF methylation at promoter IV which contains the CREB-binding site (cAMP response element-binding site) and six CpGs (CpG 1A, 1B, 2, 3, 4 & 5) as given in the scheme 4 (Kundakovic et al., 2015). The genomic co-ordinates of the amplified region are as follows: chr11:27,723,070–27,723,280, and were retrieved from UCSC Genome Browser Human February 2009 (GRCh37/hg19) Assembly (Kundakovic et al., 2015).

The human BDNF IV gene. The sequences were retrieved from UCFC with the help of the co-ordinates provided in the Kundakovic et al., 2015 article. The CREB region is highlighted in yellow and CpG nucleotides are marked with green color. The forward and the reverse primers are marked with red color and the exonic region is highlighted in grey color.

DNA extraction: For the methylation analysis, DNA was first extracted from all 25 placenta samples. 100 mg of tissue homogenate was disrupted with beads (Qiagen) and was incubated in proteinase K and DNA was extracted using the phenol-chloroform method. The concentration and purity of DNA was initially measured using NanoDrop Spectrophotometer. All the samples had approximately 1.8-1.9 ratio at 260/ 280 absorbance indicating that the extracted DNA was pure from protein contamination. Since accurate quantification of DNA is extremely important for epigenetic studies, we further measured the concentration of DNA by using QuantiFluor dsDNA system which is a highly sensitive quantification system for measuring double-stranded DNA (dsDNA); it works through the binding of a fluorescent dye to double-stranded DNA (dsDNA). The average yield of DNA from the samples were approximately 8-10 µg. DNA was run on 0.7% agarose gel and a single band was visualised.

Bisulfite conversion of DNA. Bisulfite conversion of genomic DNA, to differentiate and detect unmethylated versus methylated cytosines, is the gold standard for DNA methylation analysis. In this experiment, bisulfite conversion of DNA was conducted by using the EpiTect FastBisulfite conversion kit from Qiagen. Bisulfite treatment results in the conversion of unmethylated cytosine residues to uracil, leaving the methylated cytosine unchanged. A total of 500 ng of DNA from each sample was used for bisulfite conversion. Briefly, DNA was incubated in high bisulfite salt concentrations at high temperature and low pH. To avoid DNA fragmentation due to addition of harsh bisulfite salts, DNA Protect Buffer was added that contains a pH indicator dye and provides low pH for BS conversion. Subsequently to this, there are a series of thermal incubation steps that helps in DNA denaturation resulting in single-stranded DNA necessary for cytosine conversion. This is followed by sulfonation and cytosine deamination, and the final desulfonation step required for chemical conversion of cytosine was achieved by an on-column step during DNA purification. The BS-converted DNA was purified using Qiagen Spin columns and the final eluted DNA concentration was measured by QuantiFluor dsDNA system. The average yield of DNA after bisulfite conversion was 150 ng.

The BS-converted DNA (0.5 ng) was used for downstream HRM PCR analyses. We used EpiTect HRM PCR kit from Qiagen for the analyses. The following scheme shows the BS-converted primers that were used for HRM-PCR analysis (Kundakovic et al., 2015).

Table 8: BS-converted primers that were used for HRM-PCR analysis

Gene	Forward primer	Reverse primer
BDNF	GATTTTGGTAATTAGTGTATTA GAGTGTT	ATCAACCAAAAACTCCATTTAA TCTC

High-Resolution Melt Analysis: The EpiTect HRM kit enables the detection of methylation in the BS-converted DNA. The kit contains a mastermix with the dsDNA-binding EvaGreen dye, HRM buffer and HotStarTaq Plus DNA polymerase that helps to specifically amplify the region of interest. The HRM amplification was performed on a BioRad CFX 384 Real-time PCR system under the following conditions: a pre-incubation step at 98 °C for 5 min, 40 cycles of denaturation at 95°C for 10 s, annealing at 55°C for 30 s and extension at 72°C for 1 min, followed by the HRM analysis with increasing temperatures from 65 to 95°C in a 0.1°C/sec slope increment for 2 s. The results of the HRM were analysed by using the Precision Melt Analysis software (Bio-Rad). The clustering of the melting curves was based on the pre-melting, melting and post-melting regions.

4.6.4 RNA quality assessment

RNA was extracted to check the integrity as this is an essential factor for all the downstream applications that involves RNA. We randomly chose six INMA placenta samples (Sample Nos. 7032, 100208, 27759, 107660, 49402 and 146260) and extracted RNA by using the Qiagen RNA extraction kit (RNeasy Mini kit) by following the manufacturer's instructions. RNA concentration was measured by using NanoDrop spectrophotometer and the samples were loaded on 1% agarose gel to visualise the typical 28S and 18 S bands which is a characteristic of RNA quality.

In addition, RNA from nine INMA placenta samples (Sample Nos. 122741, 105086, 37716, 39897, 27759, 107660, 7032, 100208, 146266) was extracted by using Macherey-Nagel NucleoSpin RNA kit. RNA concentration was measured by using NanoDrop spectrophotometer and the quality of the extracted RNA was analysed by using Agilent Bioanalyser kit as per manufacturer's instructions.

5 Results

5.1 PFAS measurements in placental homogenates (INRA)

PFOS, PFOA and PFNA were detected in all the analysed samples. Typical examples of obtained diagnostic ion chromatograms for these PFAS markers in the analysed samples are given in Figure 3. Detection rates observed for PFHxS and PFDA were 96 and 68% respectively. Detection rates for other monitored PFAS markers ranged between 0 and 36%. The descriptive exposure data and related distributions are given in Table 9 only for the 5 most frequently detected compounds. The corresponding box-plot are given in Figure 4. The observed correlation between the measured PFOS and PFOA levels is illustrated in Figure 5.

Table 9: descriptive exposure data (concentrations in µg/kg) determined for the PFAS markers monitored in the 25 analysed placenta samples.

Exposure Marker	Mean	Geom.Mea	Std.Dev	Min	p5	p25	p50	p75	p95	Max
PFHxS	0.07	0.06	0.04	0.01	0.03	0.04	0.06	0.10	0.13	0.17
PFOS	0.57	0.48	0.31	0.09	0.17	0.36	0.52	0.78	1.09	1.37
PFOA	0.25	0.21	0.19	0.06	0.09	0.15	0.23	0.27	0.53	0.99
PFNA	0.12	0.11	0.07	0.04	0.04	0.08	0.11	0.15	0.23	0.34
PFDA	0.09	0.08	0.05	0.05	0.05	0.05	0.06	0.12	0.16	0.23

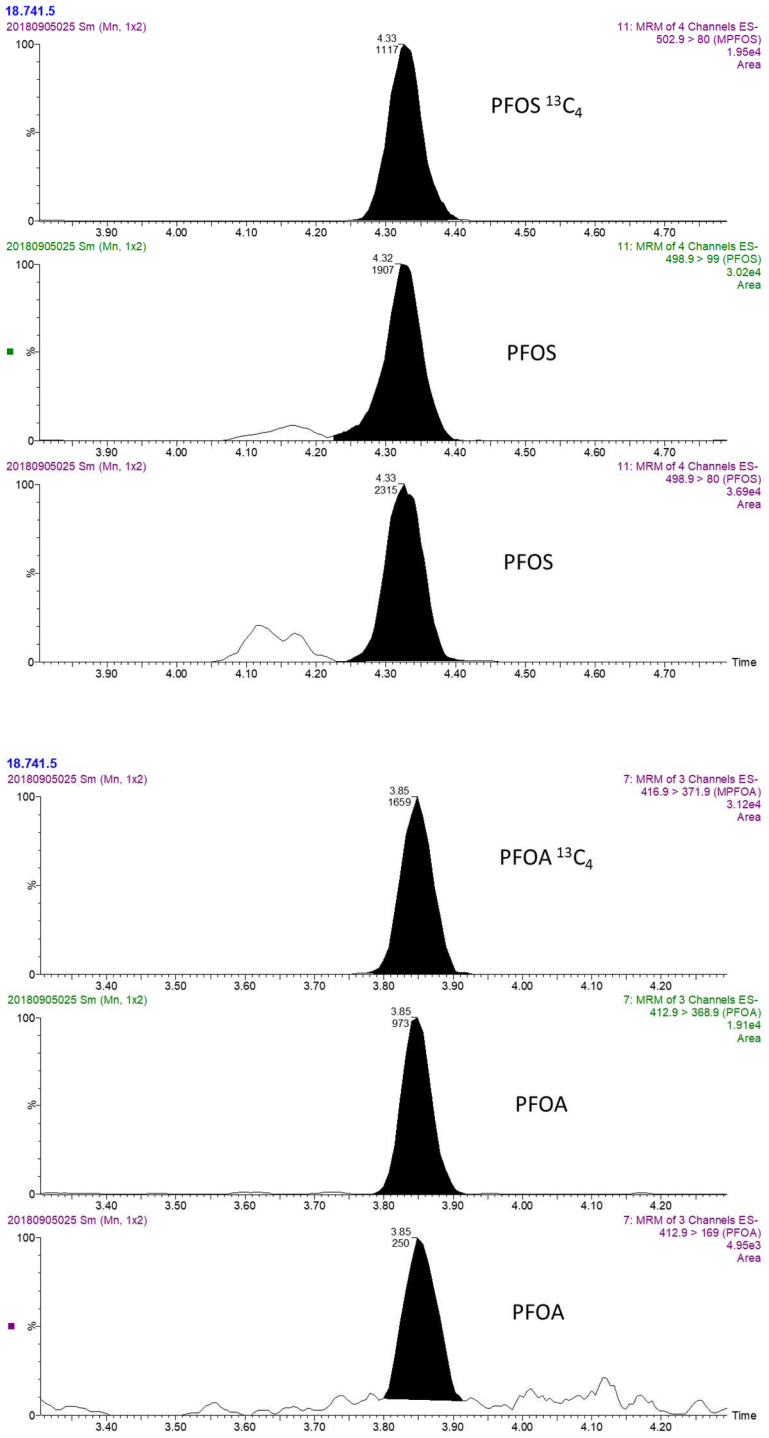

Figure 3: Typical examples of diagnostic ion chromatograms (MRM transitions) obtained in LC-MS/MS (Waters Xevo instrument, negative electrospray) for PFOS (up) and PFOA (down) in one of the analysed placenta sample

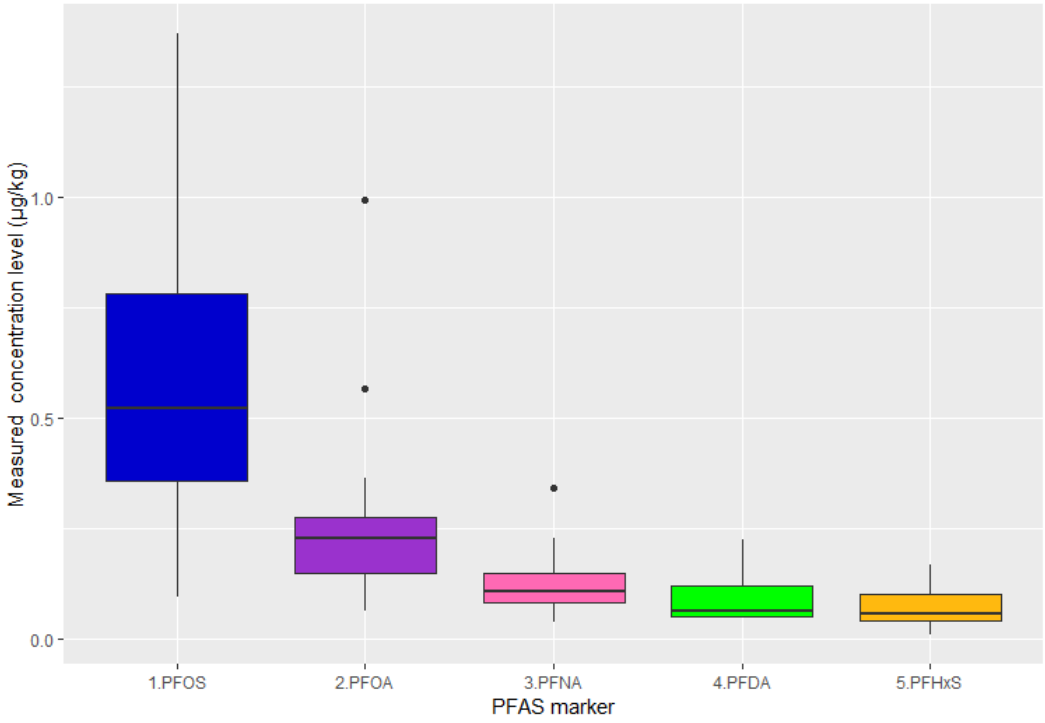

Figure 4: box-plots of the measured exposure levels for PFOS, PFOA, PFNA, PFDA and PFHxS in the 25 analysed placenta samples

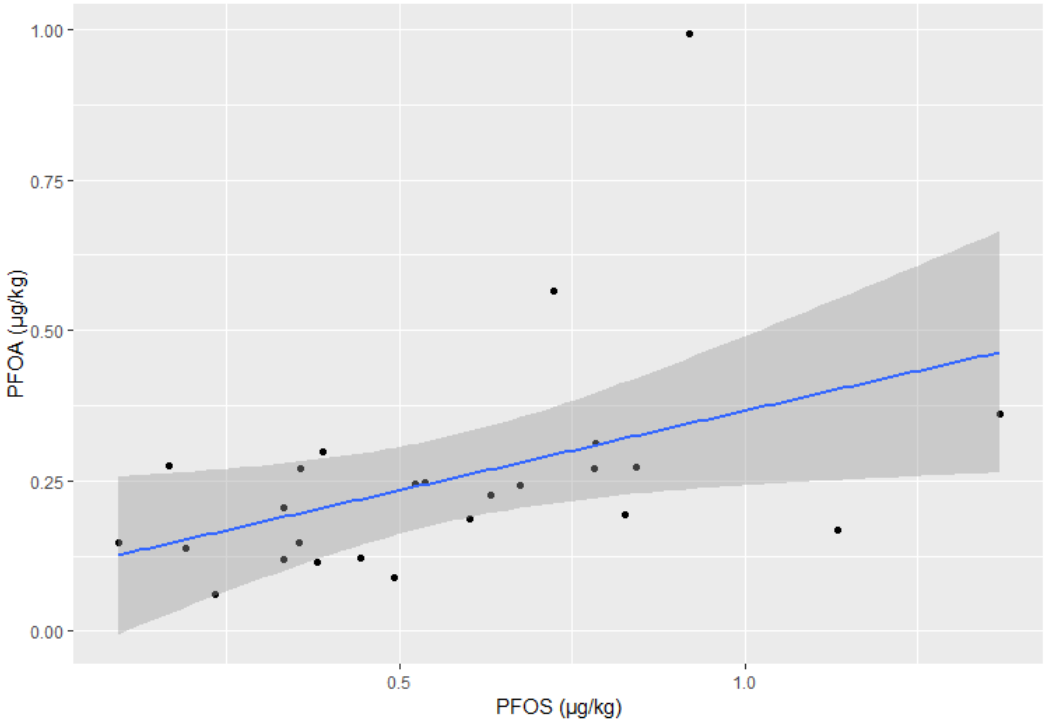

Figure 5: correlation between the concentrations of PFOS and PFOA determined in the 25 analysed placenta samples

5.2 Metal profile in placental homogenates (INSERM)

Concentrations (µg/g) of metal from placental homogenates are detailed in tables 10 and 11 as well as in Figures 6, 7 and 8, (see below).

Table 10: Metals determination in the placental samples

Determination of metals in 25 freeze-dried placenta samples															
	Zn	Cu	Se	Bi	Mn	Ba	Pb	Hg	Ag	Tl	Cd	Cs	Be	V	U
Unité	µg/g	µg/g	µg/g	µg/g	µg/g	µg/g	µg/g	µg/g	µg/g	µg/g	µg/g	µg/g	µg/g	µg/g	µg/g
LQ	2,0	0,50	0,050	0,005	0,500	0,050	0,01	0,008	0,002	0,04	0,0025	0,005	0,005	0,400	0,005
7032	46,6	7,09	1,005	<lq	<lq	0,251	0,051	0,057	0,092	<lq	0,015	0,047	<lq	<lq	<lq
10028	40,8	7,48	1,849	0,104	<lq	0,096	0,046	0,038	0,024	<lq	0,028	0,026	<lq	<lq	<lq
27759	53,6	6,43	0,916	<lq	<lq	0,257	0,041	0,063	0,004	<lq	0,028	0,033	<lq	<lq	<lq
107660	41,4	7,10	4,523	0,055	<lq	0,156	0,240	0,059	0,022	<lq	0,018	0,028	<lq	<lq	<lq
49402	42,8	6,64	1,027	0,037	<lq	0,054	0,039	0,037	0,029	0,074	0,029	0,025	<lq	<lq	<lq
146266	39,3	6,07	0,918	<lq	0,633	<lq	0,028	0,097	0,003	<lq	0,013	0,018	<lq	<lq	<lq
146433	38,3	5,51	0,952	0,017	<lq	<lq	0,017	0,019	<lq	<lq	0,011	0,033	<lq	<lq	<lq
37716	41,5	6,32	0,868	<lq	0,871	0,059	0,028	0,025	<lq	<lq	0,015	0,022	<lq	<lq	<lq
156676	42,9	4,91	1,051	0,009	<lq	0,083	0,044	0,010	<lq	<lq	0,012	0,016	<lq	<lq	<lq
105086	43,5	6,99	1,076	0,010	<lq	0,138	0,054	0,042	0,015	<lq	0,050	0,031	<lq	<lq	<lq
39897	52,1	5,17	0,926	<lq	<lq	0,195	0,038	0,071	0,005	<lq	0,011	0,031	<lq	<lq	<lq
44224	45,9	5,33	0,863	<lq	0,612	0,093	0,036	0,033	0,002	<lq	0,025	0,029	<lq	<lq	<lq
122741	47,1	6,68	0,833	<lq	<lq	0,275	0,053	0,017	0,002	<lq	0,020	0,020	<lq	<lq	<lq
C-30543	49,3	4,93	0,878	<lq	0,673	0,265	0,040	0,013	<lq	<lq	0,024	0,026	<lq	<lq	<lq
140002-T	48,5	5,37	0,923	0,006	<lq	0,127	0,027	0,029	<lq	<lq	0,022	0,035	<lq	<lq	<lq
C-135915	44,5	5,63	0,901	<lq	<lq	0,083	0,043	0,172	0,003	<lq	0,013	0,027	<lq	<lq	<lq
C-9085	46,3	6,50	0,969	<lq	<lq	0,092	0,032	0,052	<lq	<lq	0,056	0,035	<lq	<lq	<lq
C-44135	45,9	5,44	0,928	<lq	<lq	0,112	0,048	0,035	0,091	<lq	0,032	0,046	<lq	<lq	<lq
17292	35,6	6,95	0,894	<lq	1,056	<lq	0,032	0,040	0,016	<lq	0,031	0,035	<lq	<lq	<lq
76748	42,0	6,06	3,799	2,203	<lq	0,094	0,092	0,044	0,010	<lq	0,024	0,032	<lq	<lq	<lq
C-59180	44,3	5,28	0,839	<lq	<lq	0,211	0,069	0,043	0,006	<lq	0,031	0,033	<lq	<lq	<lq
145644	35,1	6,01	0,849	<lq	<lq	<lq	0,031	0,035	0,002	<lq	0,018	0,029	<lq	<lq	<lq
54472	43,5	6,11	0,913	<lq	<lq	0,058	0,021	0,052	0,012	<lq	0,009	0,025	<lq	<lq	<lq
125492	46,3	4,99	0,928	<lq	<lq	0,095	0,067	0,036	0,002	<lq	0,036	0,018	<lq	<lq	<lq
C-12939	41,4	4,91	2,228	0,597	<lq	0,061	0,039	0,040	0,004	<lq	0,034	0,023	<lq	<lq	<lq
n sample> LQ	25	25	25	9	5	21	25	25	19	1	25	25	0	0	0
Min	35,1	4,91	0,83	0,006	0,612	0,054	0,017	0,010	0,002	0,074	0,009	0,016			
Max	53,6	7,48	4,52	2,203	1,06	0,275	0,240	0,172	0,092	0,074	0,056	0,047			
Mediane	43,5	6,06	0,93	0,037	0,673	0,096	0,040	0,040	0,006	0,074	0,024	0,029			

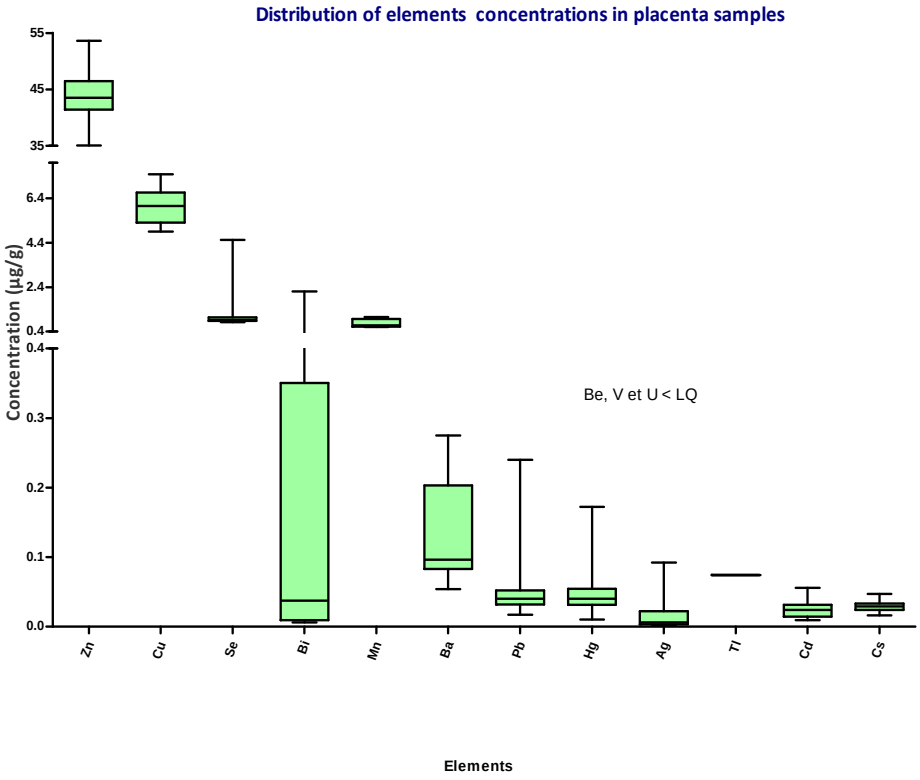

Figure 6: Distribution of the metals found in placental samples expressed in µg/g.

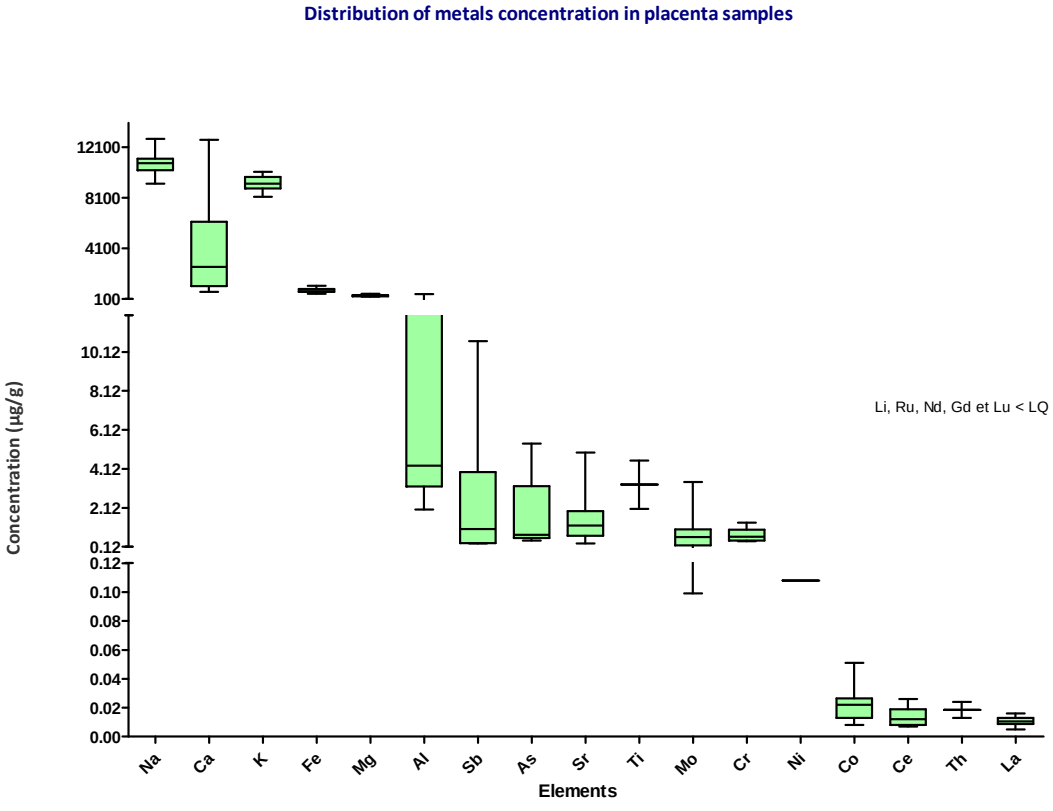

Figure 7: Distribution of the metals found in placental samples expressed in µg/g.

Table 11: Descriptive analysis of the elements tested in placental homogenates.

Elements	Na	Ca	K	Fe	Mg	Al	Sb	As	Sr	Ti	Mo	Cr	Ni	Co	Ce	Th	La	Li	Ru	Nd	Gd	Lu
Unité	µg/g	µg/g	µg/g	µg/g	µg/g	µg/g	µg/g	µg/g	µg/g	µg/g	µg/g	µg/g	µg/g	µg/g	µg/g	µg/g	µg/g	µg/g	µg/g	µg/g	µg/g	µg/g
LQ	50	50	80	2	25	2,0	0,200	0,200	0,100	2,000	0,100	0,400	0,100	0,005	0,005	0,005	0,005	0,020	0,005	0,005	0,005	0,005
n samples > LQ	25	25	25	25	25	18	6	5	25	2	8	5	1	25	11	2	6	0	0	0	0	0
Min	9220	656	8158	515	292	2,03	0,287	0,429	0,28	2,07	0,099	0,403	0,108	0,008	0,007	0,013	0,005					
Max	12742	12684	10138	1137	510	482	10,69	5,42	4,95	4,55	3,44	1,360	0,108	0,051	0,026	0,024	0,016					
Mediane	10841	2619	9222	723	354	4,28	1,03	0,74	1,21	3,31	0,623	0,630	0,108	0,022	0,012	0,018	0,010					

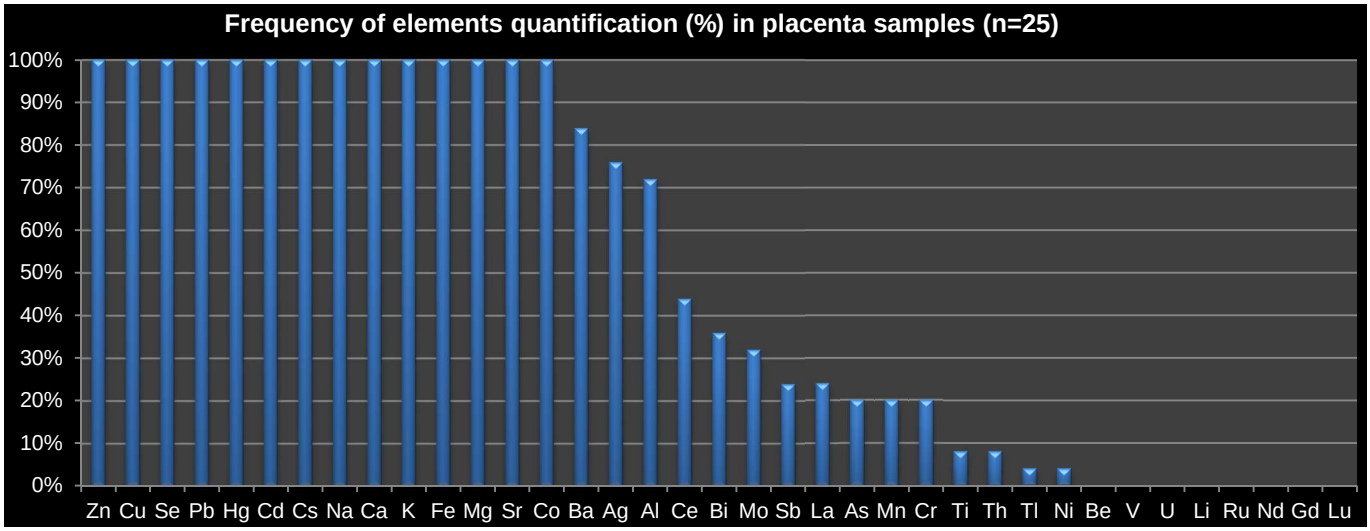

Figure 8: Frequency of the quantification in percentage of the elements found in placental samples.

5.3 Hormonal profile in placental homogenates (INRA)

Typical examples of obtained diagnostic ion chromatograms for these steroid markers in the analysed samples are given in Figure 9. Among the monitored compounds, 13 presented detection rates higher than 95% and were submitted to further data analysis. The other targeted markers exhibited detection rates between 0 and 40%. The descriptive exposure data and related distributions are given in Table 12. The corresponding box-plot (total forms) are given in Figure 10. The observed correlation between the measured free and total forms is illustrated for several target markers in Figure 11.

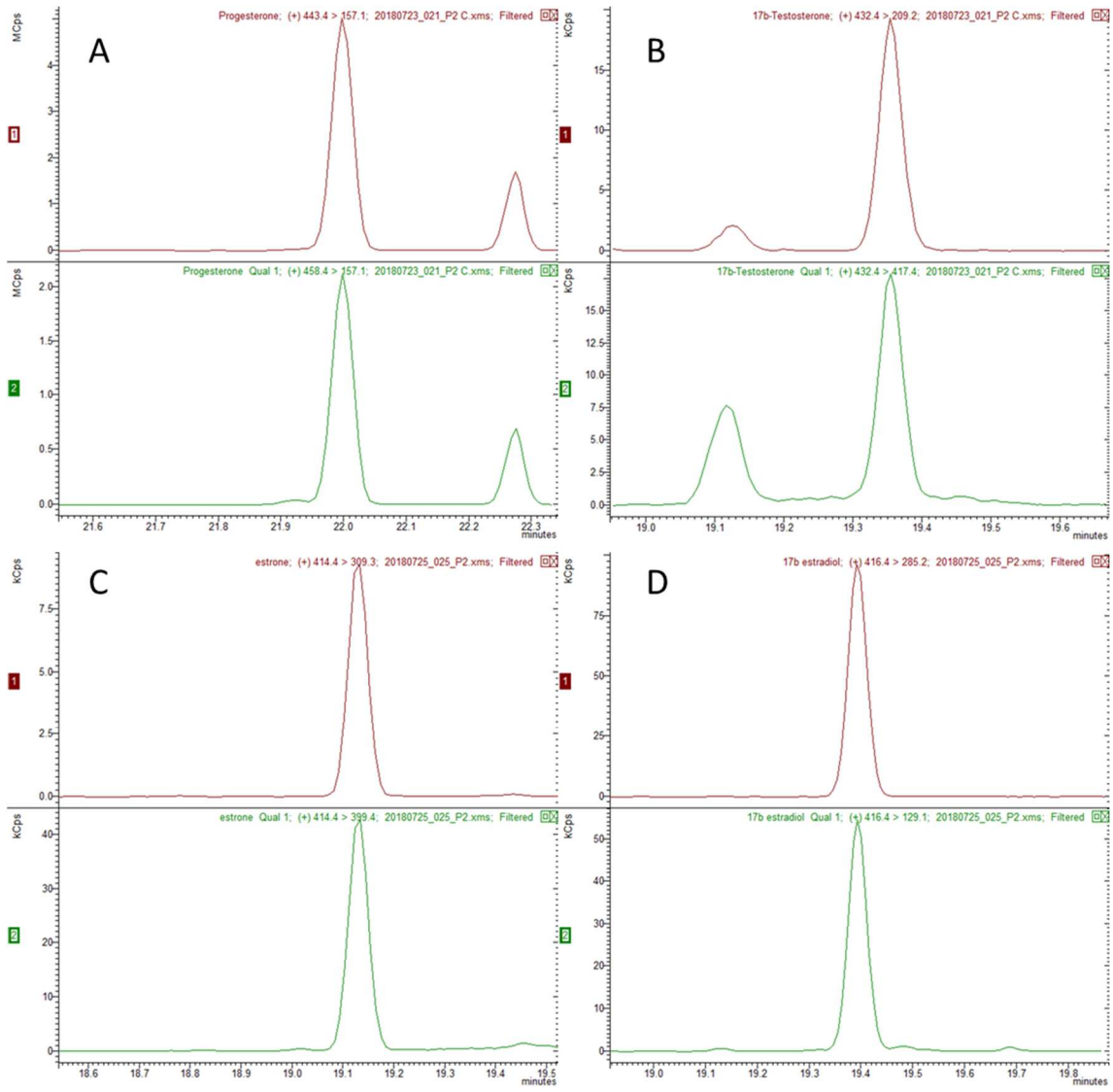

Figure 9: Typical examples of diagnostic ion chromatograms (MRM transitions) obtained in GC-MS/MS (Brucker Scion instrument, positive electron impact) for progesterone (A), 17α-testosterone (B), estrone (C) and 17α-estradiol (D) in one of the analysed placenta sample

Table 12: descriptive exposure data (concentrations in µg/kg) determined for the steroid markers monitored in the 25 analysed placenta samples

Exposure Marker	Mean	Geom.Mea	Std.Dev	Min	p5	p25	p50	p75	p95	Max
Pregnenolone_Free	116.01	111.01	33.97	47.57	69.82	97.22	109.95	134.51	177.46	191.75
Pregnenolone_Total	116.85	111.34	35.97	54.63	70.14	88.46	117.36	147.88	163.68	189.38
17aOH-pregnenolone_Free	33.98	25.92	24.07	4.96	7.36	15.18	24.37	44.45	80.05	82.24
17aOH-pregnenolone_Total	45.35	31.84	36.63	4.60	6.34	18.72	32.23	62.08	113.14	136.83
DHEA _Free	35.00	25.68	25.97	3.36	7.66	14.37	27.47	52.54	79.66	97.54
DHEA _Total	33.94	24.36	25.39	2.51	7.64	12.40	27.50	51.38	80.05	86.68
Progesterone_Free	2091.41	2048.00	441.77	1398.95	1425.06	1807.62	2016.03	2312.74	2897.16	3158.52
Progesterone_Total	1990.03	1917.88	532.47	920.73	1137.41	1700.70	1891.48	2237.43	2846.08	3160.32
17aOH-progesterone_Free	60.06	56.87	20.40	31.01	31.97	48.01	55.78	71.68	99.19	102.94
17aOH-progesterone_Total	68.82	62.31	29.74	15.11	30.93	50.82	66.72	77.56	125.13	134.31
Androstenedione_Free	32.85	25.11	22.97	4.22	5.93	17.34	26.22	41.45	70.99	87.33
Androstenedione_Total	32.24	24.20	22.72	3.35	5.31	15.38	27.03	40.25	73.37	80.76
17b-testosterone_Free	10.43	6.60	9.46	0.40	0.99	4.05	7.36	13.61	28.23	31.78
17b-testosterone_Total	9.85	6.83	8.52	0.59	1.79	4.21	6.47	13.04	25.41	32.24
Allopregnenolone_Free	65.35	62.39	19.67	33.64	34.92	51.57	63.79	79.34	98.00	101.09
Allopregnenolone_Total	227.82	214.19	81.56	116.84	118.38	159.82	210.19	289.94	361.02	433.52
Androsterone_Total	2.48	2.17	1.42	0.40	1.24	1.67	2.09	2.86	4.52	7.77
Epiandrosterone_Free	3.00	2.45	2.13	0.89	1.14	1.40	2.41	3.55	7.01	9.45
Epiandrosterone_Total	3.19	2.60	2.18	0.74	0.98	1.69	2.63	3.81	7.43	9.61
Etiocholanolone_Total	2.56	2.25	1.29	0.40	1.25	1.75	2.22	3.16	4.65	6.23
17b-estradiol_Free	75.42	67.09	41.72	32.42	35.03	51.66	57.68	96.63	152.97	205.20
17b-estradiol_Total	78.55	68.96	42.14	25.44	30.07	53.87	61.63	99.80	161.30	178.90
Estrone_Free	154.32	140.12	68.46	57.26	65.16	99.84	148.17	194.31	286.03	298.43
Estrone_Total	169.04	155.10	70.76	56.51	87.87	121.47	159.82	210.16	292.07	331.17

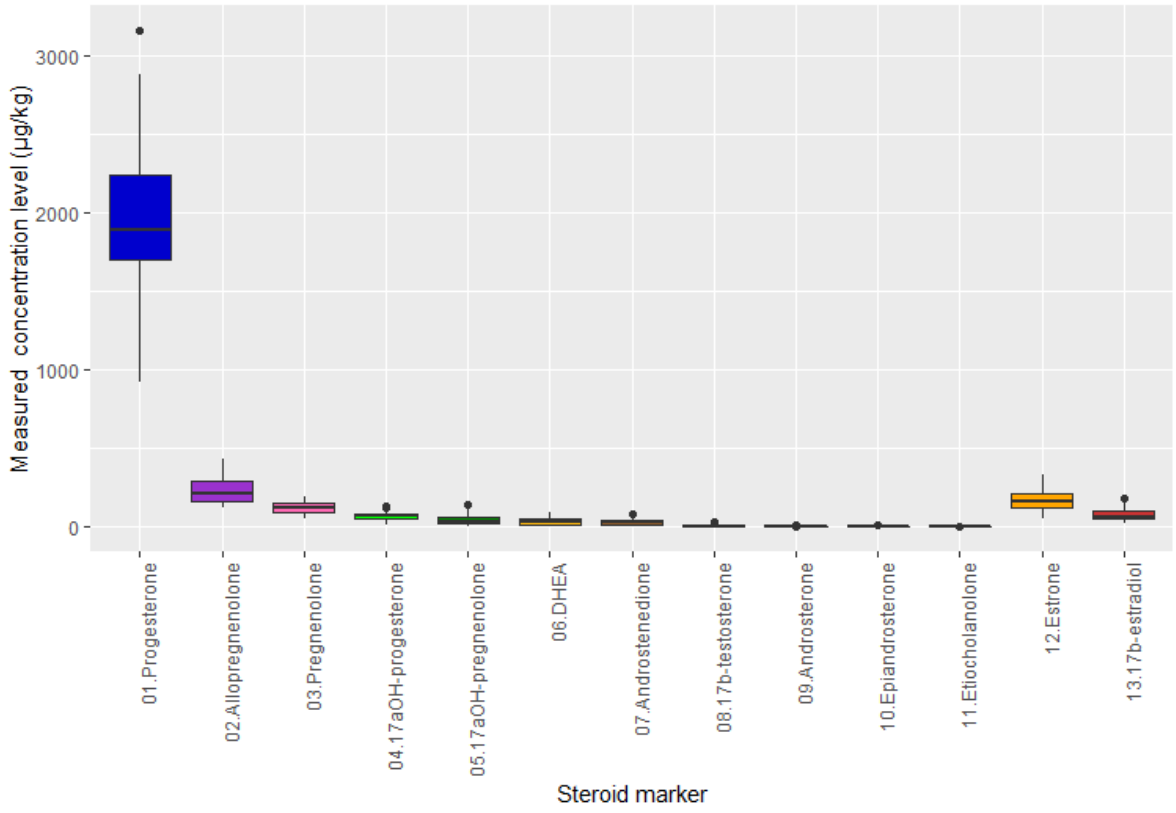

Figure 10a: box-plots of the measured exposure levels for the 13 steroids with detection rates higher than 95% in the 25 analysed placenta samples.

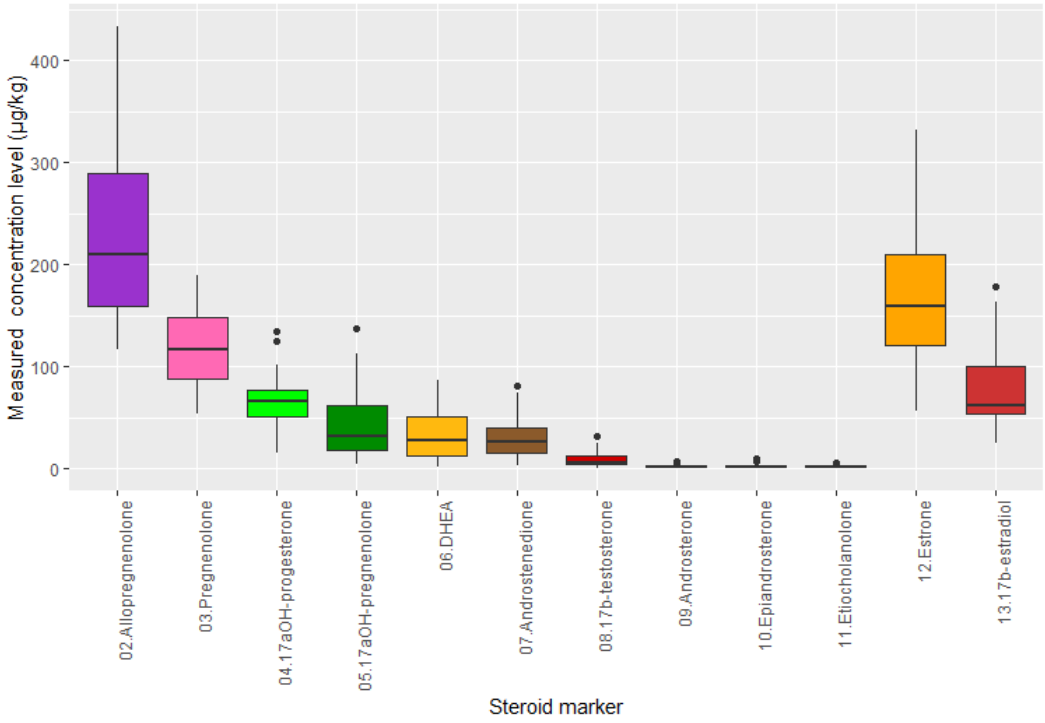

Figure 10b: box-plots of the measured exposure levels for 13 steroids with detection rates higher than 95% in the 25 analysed placenta samples (progesterone excluded for scaling reason).

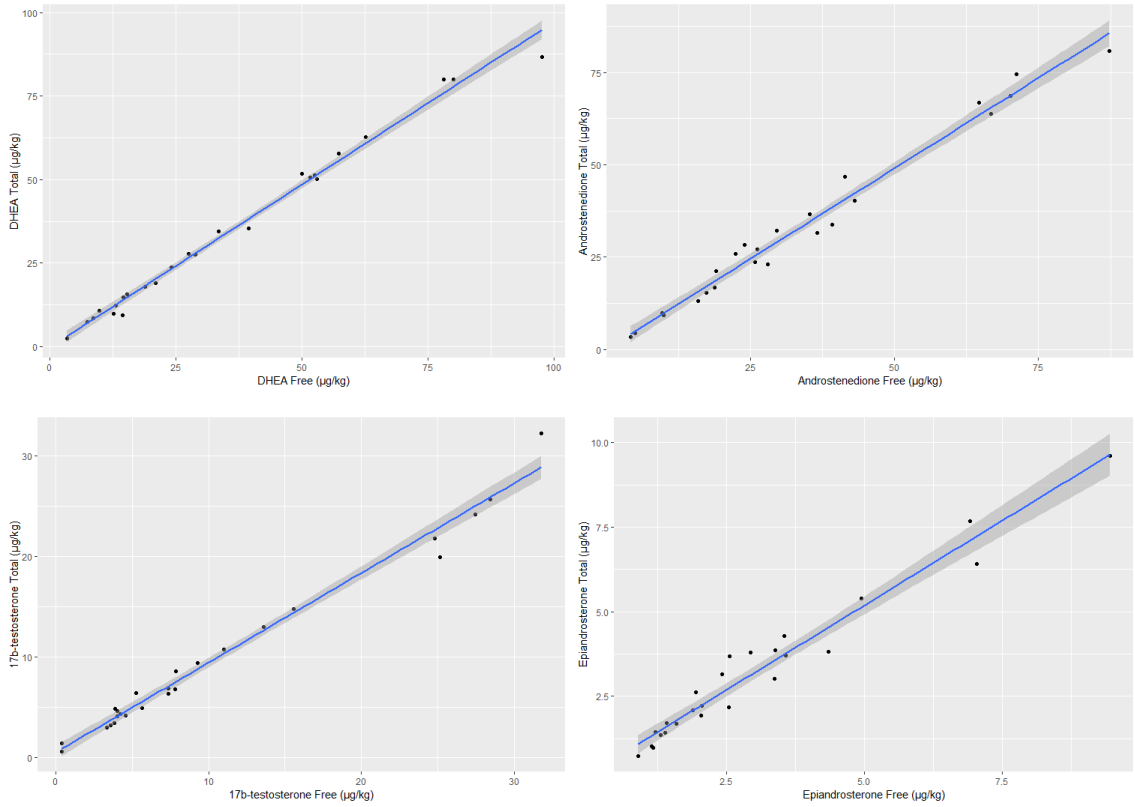

Figure 11: correlation between the concentrations of free versus total forms determined for several steroid markers in the 25 analysed placenta samples.

5.4 Untargeted metabolomics (INSERM-INRA-CEA)

Extracts of placenta (polar and non-polar fractions) from INMA birth cohort were profiled by UHPLC-ESI-HRMS (Q-TOF and Q-orbitrap) in both + ESI and -ESI modes. Principal component analysis performed on the datasets revealed that a group of ten placenta was clustering on PCAs (see Figure **12-A** as an example of PCA in positive mode for the polar fraction).

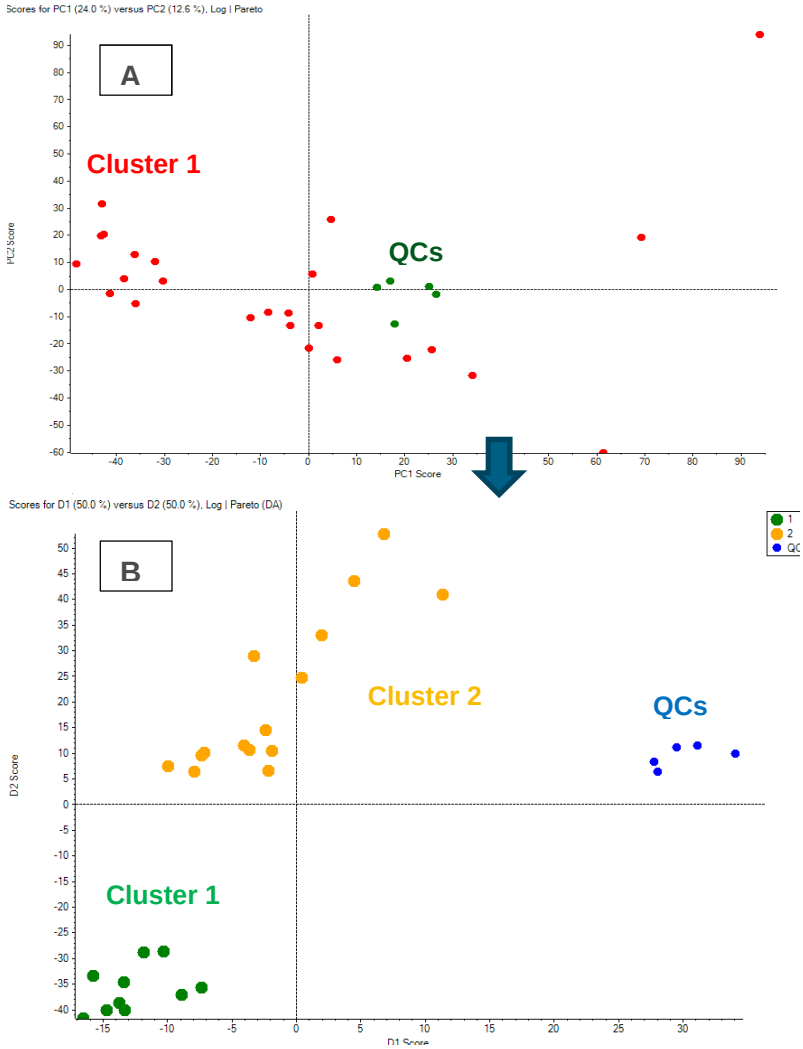

Figure 12: Results (score plot) of the non-supervised PCA based on the LC-HRMS chemical profiles generated from the polar extracted fraction of the 25 analysed placenta samples (A). Results (score plot) of the supervised PCA based on the same placenta extracts after two groups were set-up (cluster 1 comprises the 10 placentas grouping on the left of the PCA and cluster 2 comprises all the other placentas) (B). QCs= quality control. Samples were injected on the UHPLC-ESI-Q-TOF (Sciex X500R) in positive mode. Identities of placenta samples belonging to cluster 1 and 2 are presented in Table 9. QC samples comprise a composite of all samples, and were injected prior to and periodically during each analytical batch to monitor drift in instrumental response.

In these plots, the QC samples clustered together indicating that the analytical profiling methods were repeatable. As a second step, two groups were set-up from the PCAs (cluster 1 comprises a group of ten placentas on the left of the PCA and cluster 2 comprises all the other placentas) (Figure 12-B). The identities of placenta samples are presented in Table 13.

Table 13: Identity of placenta samples from cluster 1 cluster 2 as revealed by the PCA

Cluster 1	140002-T	C-12939	C-30543	C-59180	145644.00	C-90851	125492.00	
	146433.00	27759.00	C-135915					
Cluster 2	7032.00	17292.00	39897.00	122741.00	C-151676	49402.00	C-44135	
	105086.00	107660.00	146266.00	54472.00	37716.00	44224.00	76748.00	100208.00

Compounds discriminating (i.e. showing significant differences in normalised area) between clusters 1 and 2 were detected using t-test as shown in Figure 13. Following t-test, preliminary identification of compounds was done from accurate mass, isotopic fit, fragmentation data obtained from high energy collisional-induced dissociation and from comparison with in-house library or online libraries.

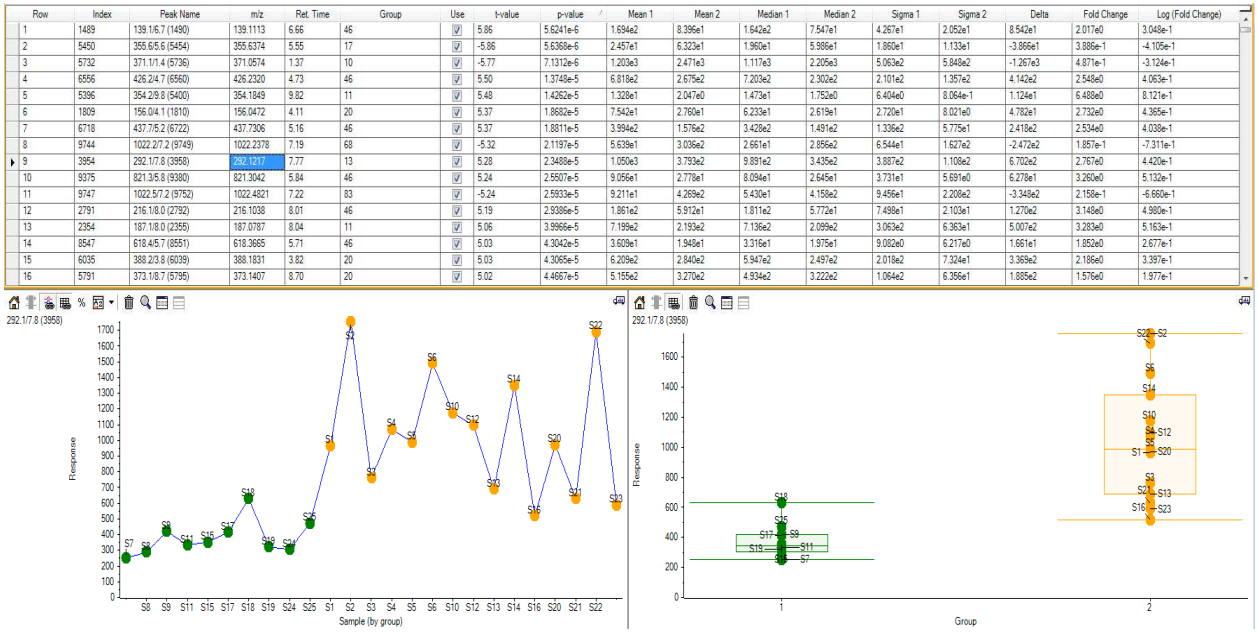

Figure 13: MarkerView t-test results showing markers (i.e. retention time x m/z variables) with significant differences in terms of normalised area between clusters 1 and 2.

A set of metabolites including 8-chloroxanthine, S-HpETE like, prostaglandin E2, prostaglandin D2, OH-prostaglandin E1 like and 19-OH-prostaglandin A2 like has been putatively identified as increasing in cluster 2 (4-10 fold change, 0.001<p-value<0.05). Identities of prostaglandin E2 and prostaglandin D2 have been confirmed using standards. A significant number of markers discriminating between clusters 1 and 2 remains to be identified between which will require further analyses.

In addition, a suspect screening using the in-house library revealed the presence of xenobiotics such as paracetamol glucuronide (1 out of 25 placenta), triclosan glucuronide (6 out of 25), caffeine (21 out of 25), lidocaine (2 out of 25), mepivacaine (18 out of 25), bupivaciane (9 out of 25) in some of these placenta samples. Further work on annotation could provide more information on biomarkers of exposure present in these placentas.

5.5 Anti-androgenic activity of placental alpha fractions (DTU)

5.5.1.1 *AR antagonistic activity*

The controls R1881 (known AR agonist) and OHF (an AR antagonist) was tested alongside the placenta extracts in each independent experiment and gave and the expected increase and inhibition, respectively of AR activity with EC_{50} of 0.05nM for R1881 and IC_{50} of 27.3 nM for OHF (**Figure 14**).

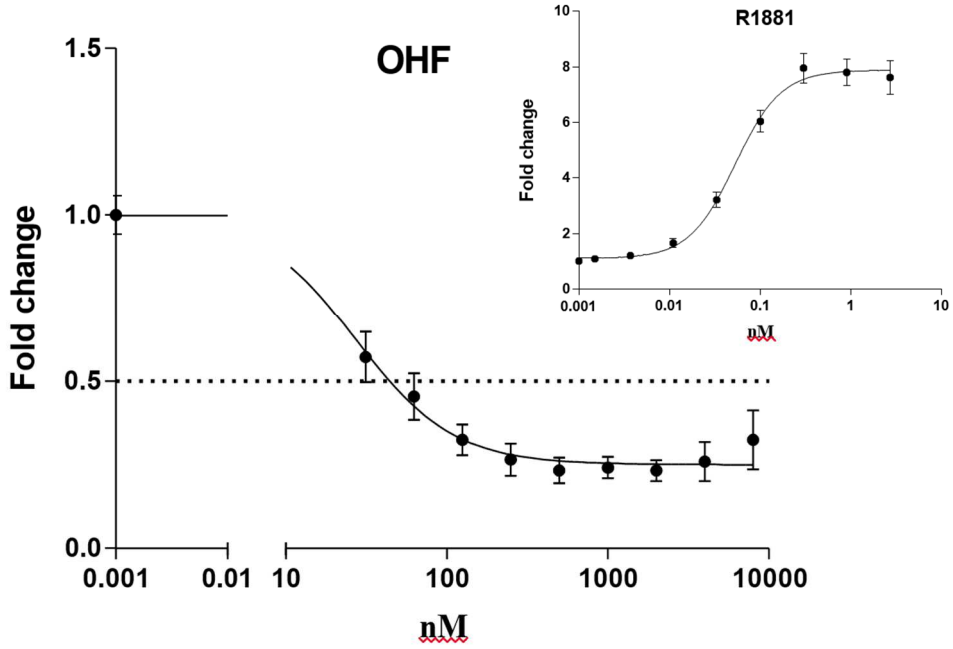

Figure 14: Concentration-response curves for the AR agonist R1881 and the AR antagonist control OHF. Data presents mean ± SD for three independent experiments. The Four parameter logistic curve fits were made in Graph Pad Prism 5 and the respective EC50 value of 0.05 nM and IC50 value of 27.3 nM were derived from these curves.

All 24 placenta extracts were tested for AR antagonistic in three dilutions (x60, x180 and x600). AR antagonistic activity was observed for all 24 extracts, but to varying degrees (Figure 15). The inhibition of AR activity was concentration dependent and for all 24 extracts the effect was most pronounced in the least diluted extract (x60) (Figure 15).

Table 14 shows the ranking of the 24 extracts according to their maximum % inhibition of AR activity at the second lowest (non-cytotoxic) dilution of 1.7 mg/well (180- times diluted), compared with the maximum effect seen at the lowest dilution of 5 mg/well (60-times diluted). At the second lowest dilution of 1.7 mg/well the maximum effect is ranging from 26-27% for the three most potent extracts: no. 5 > 7 > 1 respectively. If one excludes the extracts where cytotoxicity were judged, maximum effects were seen at 5 mg/well (60-times diluted), ranging between 86-69% inhibition of AR activity for the three most potent extracts: no. 11> 14 > 15, respectively. The least potent extract was extract no. 21 at 180-times diluted and extract no. 6 at 60-times diluted (ranking 20th at x180).

Figure 16 shows the results from the cytotoxicity measurements. As can been seen from figure 14 it seems that something in the placental fractions is affecting or influencing the Renilla luciferase leading to an increase in luciferase activity. Because of this overall increasing effect of the placental extracts compared to the control in the cell viability assay, it was decided to judge cytotoxicity as decrease in luciferase activity of >20% compared to the lowest dilution (x600) of each extract instead of comparing to the media control.

Based on this approach cytotoxicity was observed for extract 1, 7, 8, 9, 12 and 16 at the lowest dilution of 60 times (indicated by a “C” in figure 13).

Table 14: Placenta extracts ranked according to AR antagonistic potency for the most concentrated and second most concentrated dilutions

Extract number	Max (%) inhibition at 180-times dilution (1.7mg/well)	Max (%) inhibition at 60-times dilution (5mg/well)
EXT5	**27.3%**	54.6%
EXT7	**26.6%**	84.3%*
EXT1	**25.8%**	80.7%*
EXT11	25.1%	**86.4%**
EXT9	24.3%	86.3%*
EXT16	22.5%	87.8%*
EXT8	19.6%	82.6%*
EXT4	19.3%	50.2%
EXT15	18.4%	**69.1%**
EXT12	17.7%	81.2%*
EXT14	14.2%	**75.9%**
EXT10	14.1%	56.0%
EXT17	13.0%	58.0%
EXT18	12.8%	50.1%
EXT13	12.2%	36.1%
EXT19	11.3%	45.4%
EXT2	10.9%	43.6%
EXT23	8.5%	54.5%
EXT22	7.7%	57.5%
EXT6	7.3%	**32.0%**
EXT25	5.7%	38.3%
EXT24	4.9%	54.1%
EXT20	2.0%	54.5%
EXT21	**0%**	35.9%

Red, **blue** and **green** colour illustrate 1; 2; and 3 ranking based on % inhibition in the AR antagonist assay.

*: cytotoxicity defined as a decrease in cell viability of >20% was observed and therefore these values were not included in the ranking. The dark orange illustrate the lowest % inhibition found for the respective dilutions (180- or 60-times)

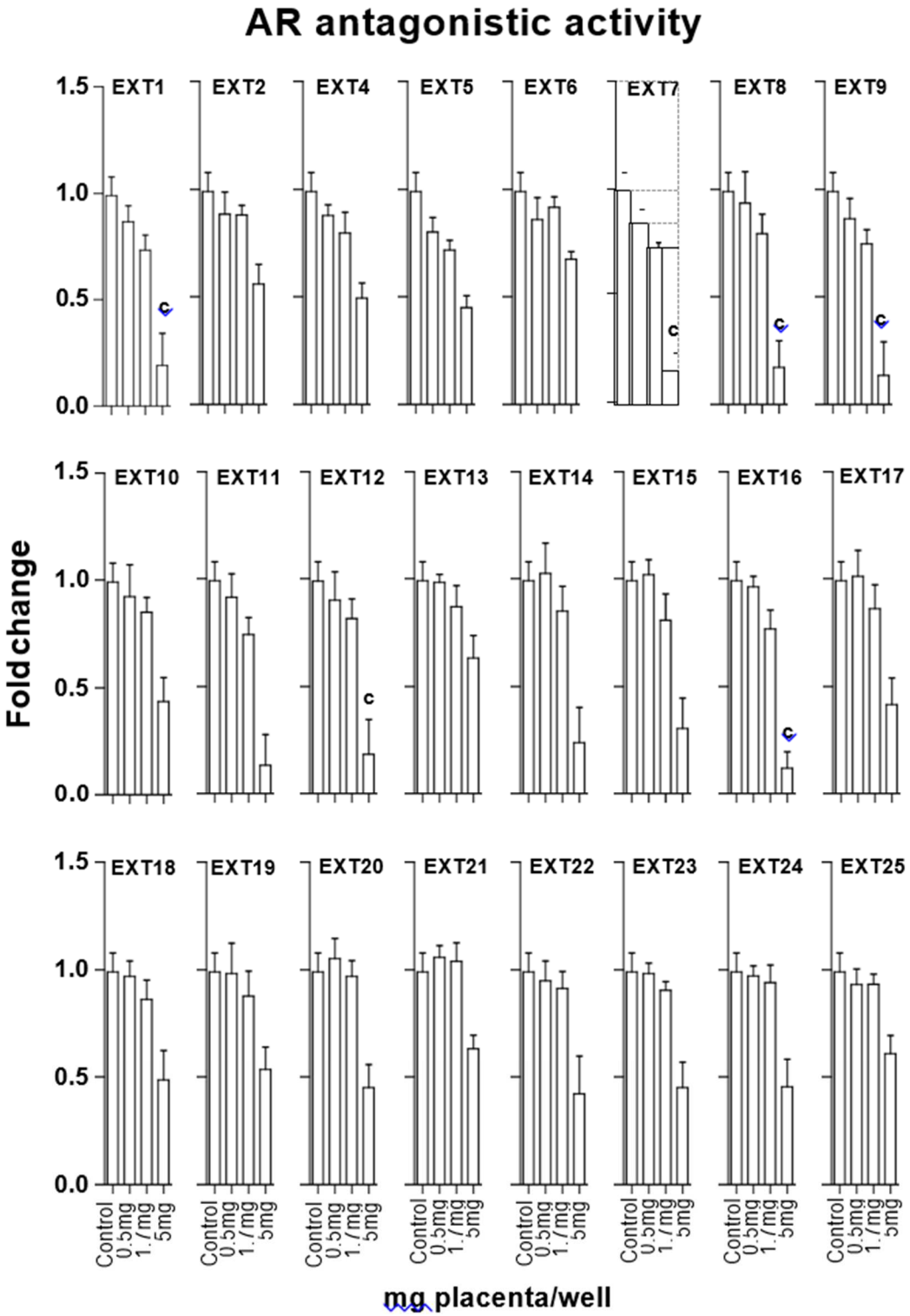

Figure 15: AR antagonistic activity of placenta extracts dilutions of 600, 180, and 60 times equivalent to 0.5 mgplacenta/well, 1.7 mgplacenta/well, and 5 mgplacenta/well, respectively. Data represents the mean ± SD from three independent experiments. All placenta dilutions were tested in triplicates and normalized to medium controls pooled from all plates. EXT=extract. C= cytotoxicity evaluated as the pooled data from the three independent experiments.

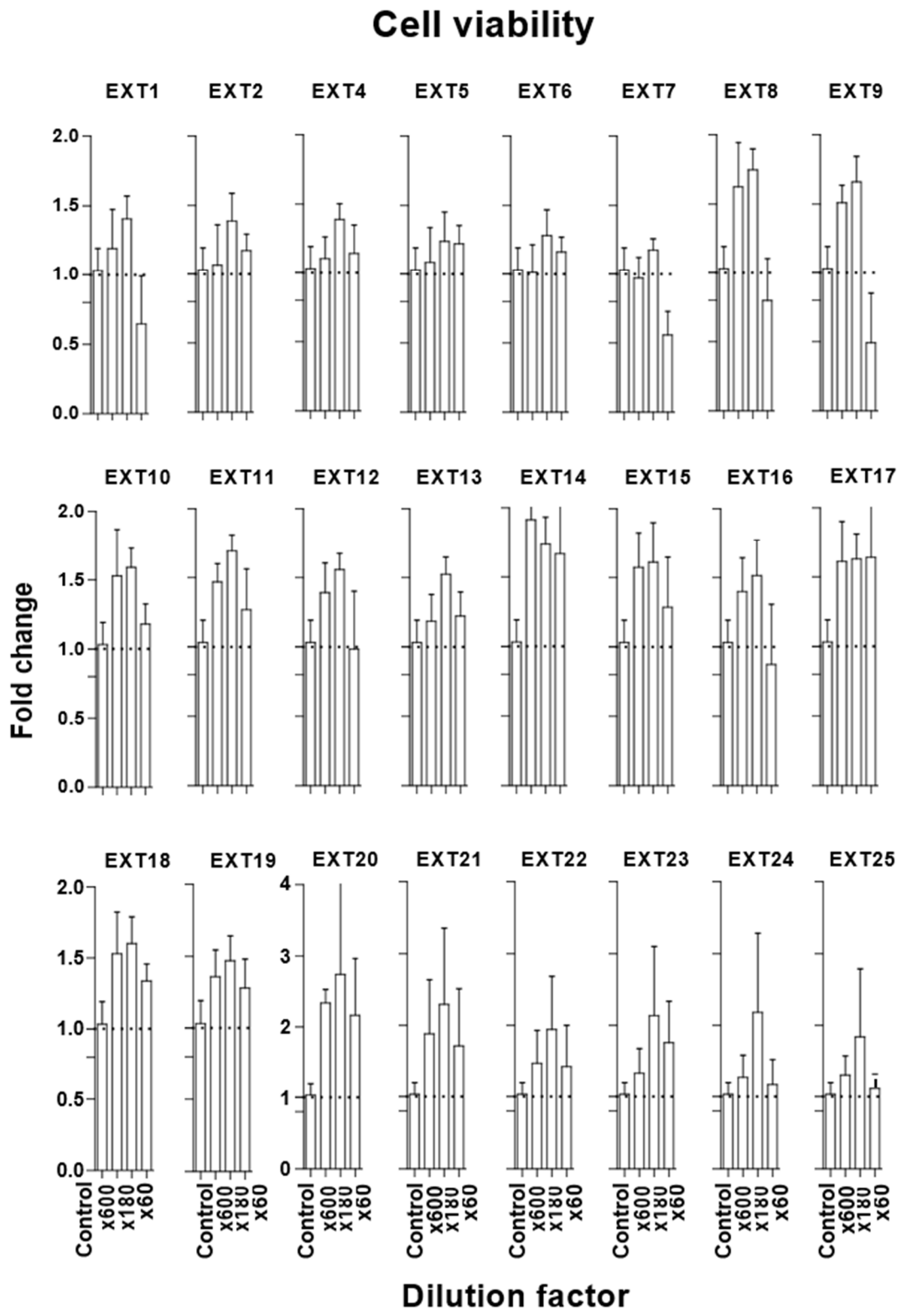

Figure 16: Cell viability of placenta extract dilutions of 600, 180, and 60 times equivalent to 0.5mg placenta/well, 1.7 mg placenta/well, and 5mg placenta/well, respectively. Data are from three independent experiments and presented as mean ± SD. All placenta dilution were tested in triplicates and normalized to medium controls pooled from all plates. EXT=extract

5.6 Urinary measurements for 8-OHdG (MU)

Concentrations of measured OH-dG in urine samples are showed in **Table 15** and **Figure 17**.

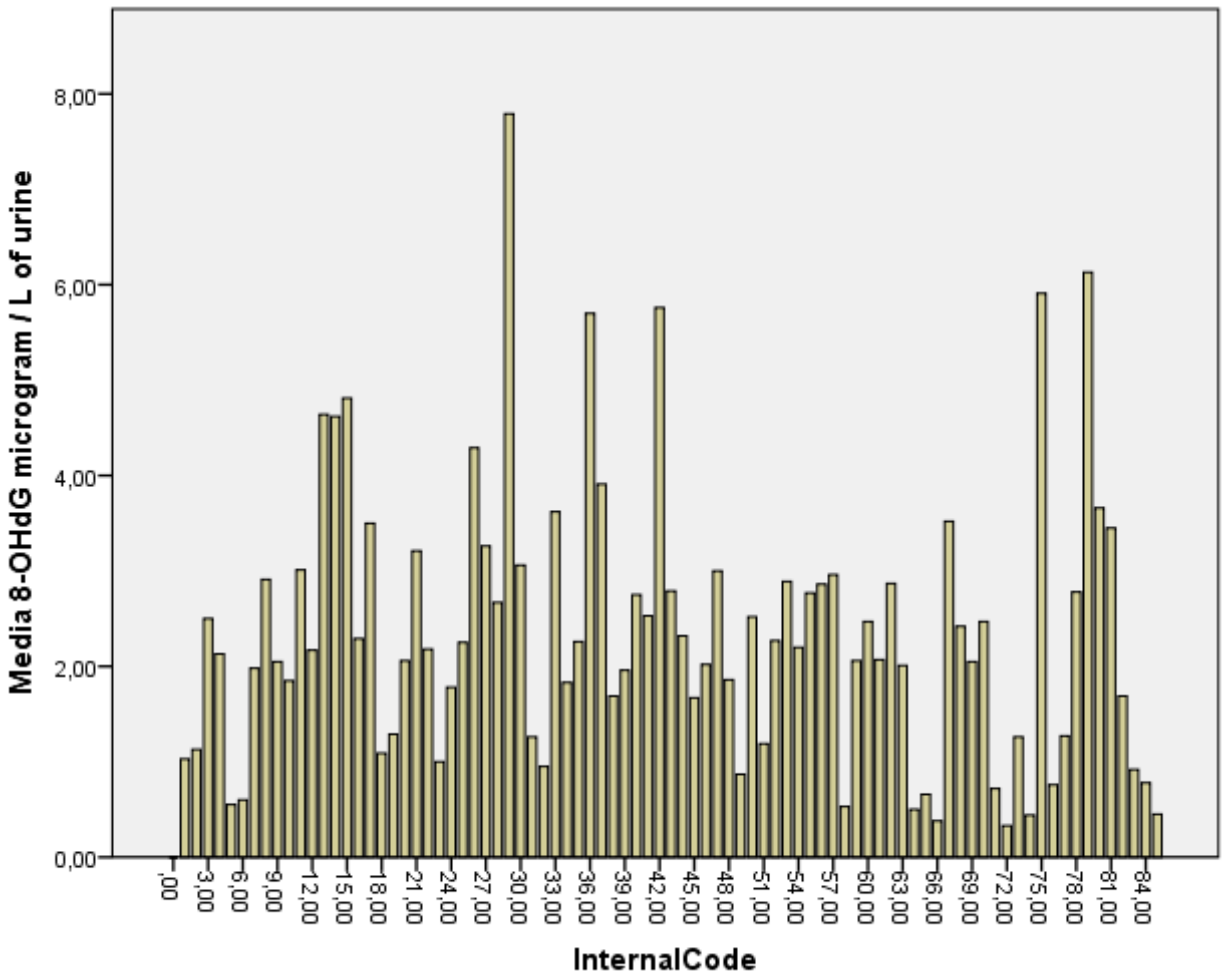

Figure 17: Urinary 8-OHdG concentrations measured by Masaryk University using LC-MS/MS.

Table 15: OH-dG concentrations in urine samples

Internal codes-urine	8-OHdG microgram / L of urine	8-OHdG microgram / gram of creatinine	Creatinine milligram / L of urine	Continuation: Internal codes-urine	8-OHdG microgram / L of urine	8-OHdG microgram / gram of creatinine	Creatinine milligram / L of urine
1	1,03	3,7	277	43	2,79	6	463
2	1,13	3,1	370	44	2,32	4	582
3	2,5	4,5	552	45	1,67	3,9	422
4	2,13	4,7	448	46	2,02	6,3	322
5	0,55	2,4	231	47	3	6,1	493
6	0,6	1,7	358	48	1,86	6,6	283
7	1,98	10,5	189	49	0,87	3,2	275
8	2,91	3,9	755	50	2,52	3,5	718
9	2,05	3,7	557	51	1,19	2,5	467
10	1,85	7,9	235	52	2,27	5,7	396
11	3,01	4,3	693	53	2,89	6,5	444
12	2,17	5,1	425	54	2,2	5,1	433
13	4,64	7,6	610	55	2,77	4,7	589
14	4,62	3,6	1270	56	2,86	7,3	394
15	4,81	4,8	998	57	2,96	7	423
16	2,29	2,9	781	58	0,53	2,3	229
17	3,5	6,6	527	59	2,06	3,7	560
18	1,09	2,8	393	60	2,47	4,1	608
19	1,29	2,7	471	61	2,07	4,5	462
20	2,06	3,5	593	62	2,87	7,4	387
21	3,21	5,6	573	x	not available	not available	not available
22	2,18	6,7	328	63	2,01	4,8	414
23	1	3,5	285	64	0,5	2,8	180
24	1,78	4,4	402	65	0,66	3	217
25	2,25	5,1	445	66	0,38	2,3	162
26	4,29	10,1	426	67	3,52	4,9	722
27	3,26	6,9	476	68	2,42	3,5	694
28	2,67	4,4	608	69	2,05	3,8	542
29	7,79	13,1	594	70	2,47	6,6	372
30	3,06	6,7	457	71	0,72	3	240
31	1,26	2,7	472	72	0,33	3,6	92
32	0,95	2,6	372	73	1,26	2,9	427
33	3,62	5,5	657	74	0,44	2,5	175
x	not available	not available	not available	75	5,91	7,8	754
34	1,83	3,5	518	76	0,76	2,2	350

Internal codes-urine	8-OHdG microgram / L of urine	8-OHdG microgram / gram of creatinine	Creatinine milligram / L of urine	Continuation: Internal codes-urine	8-OHdG microgram / L of urine	8-OHdG microgram / gram of creatinine	Creatinine milligram / L of urine
35	2,26	9,8	231	77	1,27	1,7	747
36	5,7	10,1	564	78	2,78	5,9	472
37	3,91	7,8	502	79	6,13	8,3	737
38	1,69	5,5	308	80	3,66	7,7	475
39	1,96	3,6	539	81	3,45	4,3	805
40	2,75	5,6	488	82	1,69	42	403
41	2,53	5	505	83	0,92	3,8	240
42	5,76	6,4	900	84	0,78	4,8	162
				85	0,45	1	437

5.7 Epigenetics Biomarkers (INSERM)

5.7.1 Histone H2AX Phosphorylation (Gamma-H2AX)

The intensity of the Western blot bands was measured at least 3 times for gamma-H2AX and Ponceau-stained images by using ImageJ software. The average values from three measurements were normalised against the corresponding average values from Ponceau image measurements. A graph was plotted (Microsoft Excel) which represents the normalised values for gamma-H2AX against Ponceau for each samples (**Figure 18**). Subsequently, we classified the samples into four clusters (unsupervised clustering) based on the different ranges of normalised values. The samples whose normalised expression was <1 was classified into 1st cluster (blue), <2 was classified into 2nd cluster (orange), <3 was classified into 3rd cluster (brown) and >3 was classified into the fourth cluster (black). The samples in each cluster are provided in **table 16**. The average value of the lowest cluster was set as 1 and the relative fold increase in rest of the clusters with ± SD are shown in **Figure 19**. The t-test was used for statistical analyses and the differences were considered significant at p< 0.05 (*), p< 0.01 (**) and p< 0.001 (***).

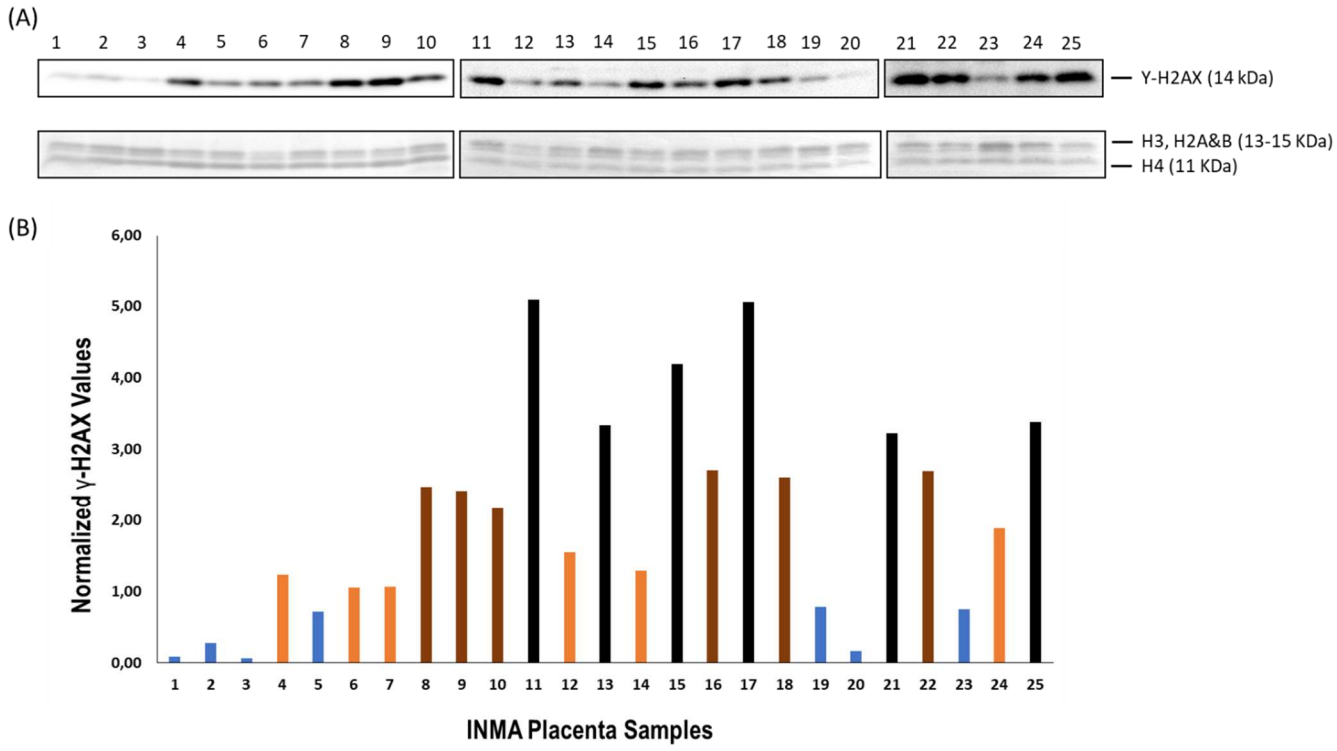

Figure 18: (A) The western blot images showing the gamma-H2AX protein levels and the corresponding ponceau-stained images. The samples that correspond to the numbers 1-25 in each lane are provided in the table (B) Graphs showing the normalised expression of gamma-H2AX against ponceau–stained H4 protein (C) Unsupervised clustering of the samples depending on the fold increase in gamma-H2AX protein levels. Table 1 shows the samples that are grouped in each cluster.

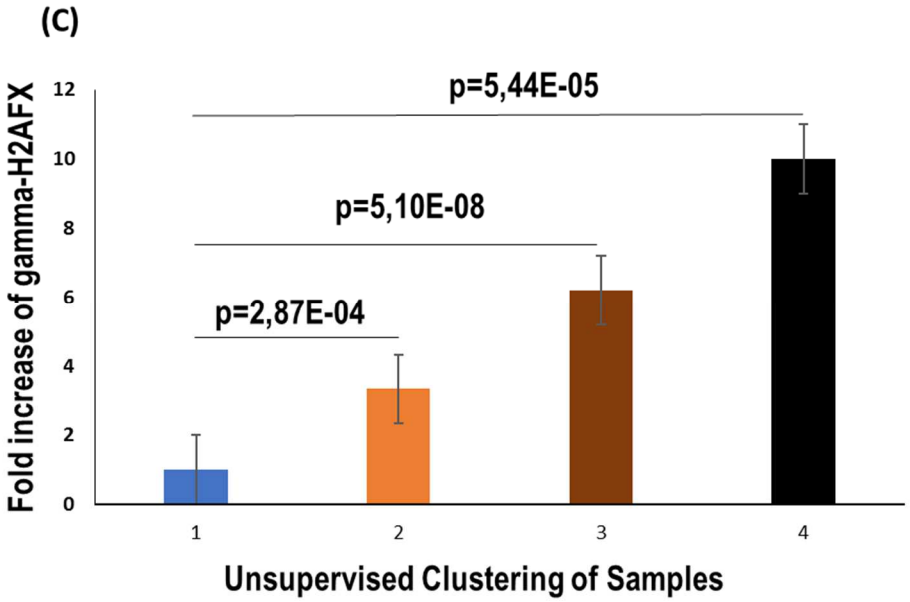

Figure 19: Unsupervised Clustering of samples

Table 16: The samples that were grouped in each cluster is as follows:

Clusters	Sample Nos.
Cluster 1	7032, 100208, 27759, 49402, 17292, 76748, 54472
Cluster 2	107660, 146266, 146433, 44224, C30543, 125492
Cluster 3	37716, C151676, 105086, C135915, C44135, 145644
Cluster 4	39897, 122741, 140002T, C90851, C59180, C12939

Smoking during pregnancy or other conditions such as preeclampsia has been reported to increase the levels of this protein in placenta.

5.7.2 Trimethylation of histone 3 at lysine 4 (H3K4me3)

The data was analysed with the help of Bio-Rad CFX Manager software. A good melt curve with a single amplicon could be observed for all the PCR products indicating the specificity of the primers and the absence of primer-dimers. We used as negative control, the region of *GAPDH* gene that is located far from the transcription start site. The normalised gene expression data with *GAPDH* as the reference gene was obtained. The basic measurement of ChIP experiment functioning is “immunoprecipitation efficiency” or “ChIP: input ratio” for a given genomic region, which is defined as the amount of PCR product in the ChIP sample divided by the amount of PCR product in the input sample. There was high enrichment in all the samples indicating the efficiency of ChIP experiment. The average ChIP values for each gene from cluster 1 and cluster 4 was calculated (Figure 20). The data were expressed as normalised ChIP fold changes when compared to the cluster 1 with ± SEM. The t-test was used for statistical analyses and the differences were considered to be significant at $p< 0.05$ (*), $p< 0.01$ (**) and $p< 0.001$ (***). The data were processed and plotted by using Microsoft Excel.

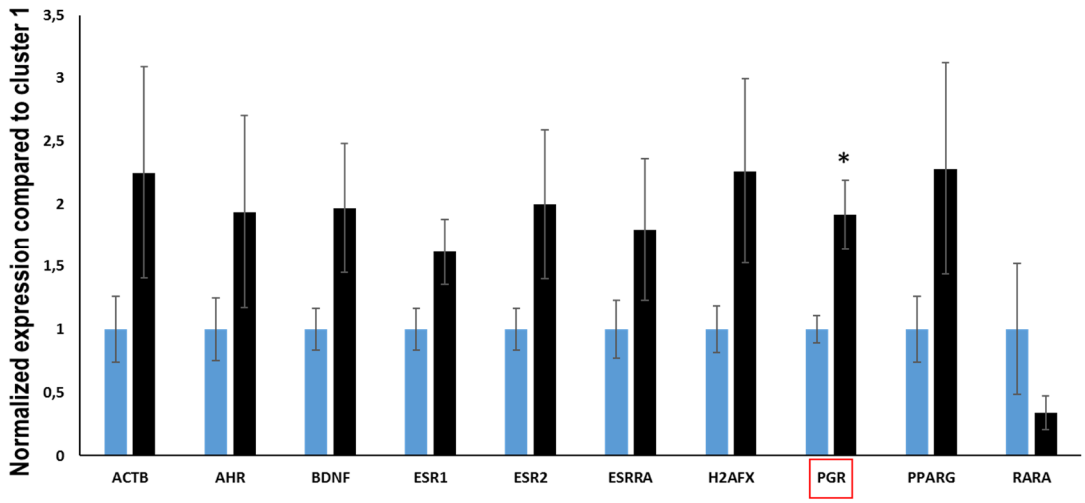

Figure 20: The graph represents the average values from cluster one (blue) and cluster 4 (black) for each gene normalised against *GAPDH*. Progesterone receptor (PGR) showed significant promoter H3K4me3 occupancy (p value = 0.02) when compared to the cluster 1. All other samples in cluster 1 showed an increase when compared to cluster 4 although there was no statistical significance. Retinoic acid showed decreased levels when compared to cluster 1.

The p-value was significant only for progesterone receptor (PGR) with a p value of 0.02 (*). It has been shown that, in humans, placenta plays an important role in progesterone synthesis unlike *corpus luteum* in other species (Feinshtein et al., 2010). Moreover, in humans, progesterone levels continuously rise until the end of pregnancy with no apparent drop in their levels during labor process (Feinshtein et al., 2010). This might explain observed increase in H3K4me3-enriched increase in PGR in placentas. On the other hand, increased levels of progesterone during pregnancy has been linked to immune suppression and disease susceptibility (Robinson and Klein, 2012).

ESR1 exhibited a p-value of 0.08 indicating trends of significance. Higher sample numbers may be required to confirm this. The data were re-analysed with Mann-Whitney test (RStudio) and was found to be significant only for PGR (p value- 0.03). The rest of the genes that were tested were not statistically significant even though all them showed a tendency to increase compared to cluster 1 except retinoic acid receptor (RARA) which showed a decrease when compared to cluster 1 though not statistically significant. The variation between samples for each gene were low in cluster 1 compared to cluster 4 suggesting less technical variability.

5.7.3 DNA methylation of BDNF

HRM Principle: Before discussing the results, we will provide an overview on how HRM works. HRM is a post-PCR method that requires a real-time PCR system with excellent thermal stability and HRM-dedicated software. HRM starts with the PCR amplification of the DNA region of interest in the presence of dsDNA-binding EvaGreen dye. The dye has high capacity to fluoresce when bound to dsDNA and it emits low fluorescence when it is in an unbound state. The PCR amplification is followed by a high resolution melting step wherein, with increasing temperature, the dsDNA dissociates (melts) into single strands thereby releasing the dye causing a change in fluorescence. The real-time PCR system captures the fluorescent change vs. change in melting temperature (T_m) with high precision and plots it as a melt curve. Although melt curves are

commonly used in qPCR experiments to ensure primer specificity and usually involve temperature range of 65-95°C in 0.5°C increments, HRM data are collected at more narrow temperature increment, 0.1-0.2°C increment. Finally, the HRM software is used to identify the pre-and post-melt fluorescence intensity, and the signals are normalised to relative values of 1 and 0 that eliminates background fluorescence thereby increasing the possibility of detecting subtle melt curve differences.

During the bisulfite treatment of DNA, all the unmethylated cytosine residues are converted to uracil, and during the PCR amplification step of HRM, they will be amplified as thymine (**Figure 21**). Only the methylated cytosines will be amplified as cytosines as shown in the figure 3 below. Hence, there is a high GC content in methylated DNA when compared to the unmethylated ones. Since the GC residues are linked by triple bonds in contrast to the double bonds of AT residues, higher temperature is required to break the GC bonds, and this creates a temperature/ fluorescence shift in the melt curves formed during HRM.

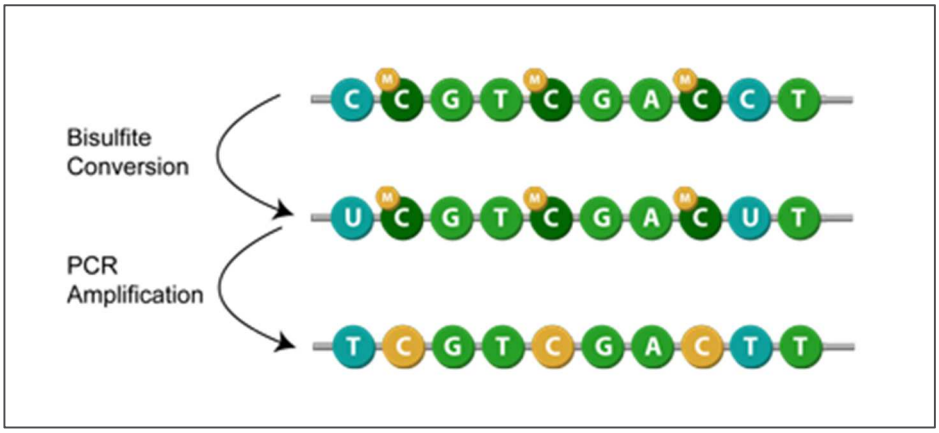

Figure 21 shows the changes that methylated and unmethylated cytosines undergo during bisulfite conversion and PCR amplification (Source: https://www.epigentek.com/catalog/dna-bisulfite-conversion-c-75_21_47.html).

Results of this study: The PCR amplification of the samples provided a good melting curve indicating that a single amplicon has been generated which denotes the BDNF primer specificity and absence of primer-dimers.

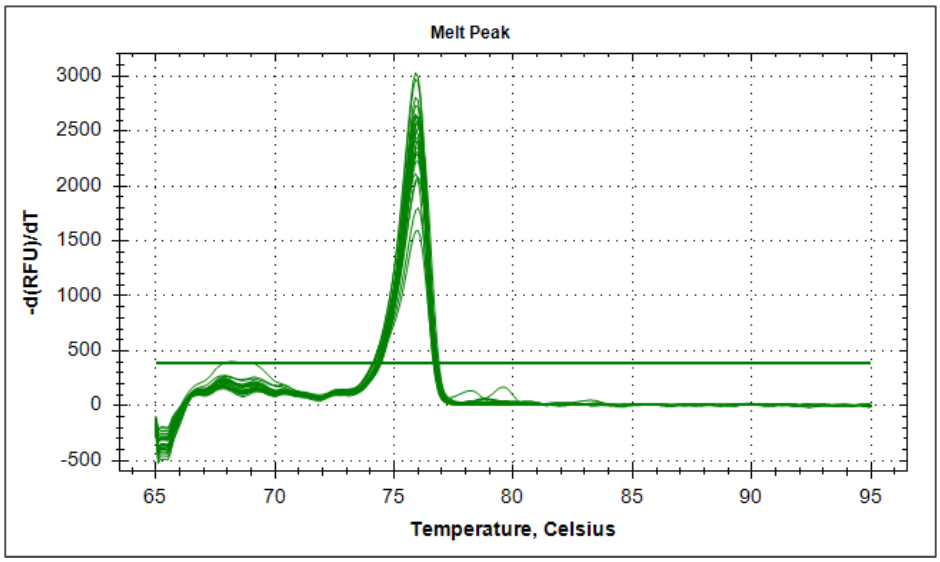

Figure 22: The PCR amplification melt curve showing single peak for BDNF indicating primer specificity and lack of primer-dimers (primer-dimers are the primer molecules that have attached to each other due to strings of complementary bases in forward and reverse primers).
The HRM PCR amplification distributed the samples into four different clusters based on the temperature and fluorescence signals generated (Figure 23 A, B & C).

Cluster 1: The following 18 samples were grouped into one cluster by the Precision Melt Software (Sample Nos. 7032, 100208, 27759, 107660, 49402, 146266, 146433, 37716, C151676, 39897, 44224, 122741, 140002-T, C135915, C90851, C44135, 17292, C59180). The average melt temperature (T_m) of this cluster was 74.57ºC

Cluster 2: The following 4 samples belonged to the second cluster with an average melting temperature of 70.02ºC (Sample Nos. 105086, C30543, 76748, C12939).

Cluster 3: The following 2 samples belonged to the third cluster which had an average melt temperature of 69.95ºC (Sample Nos. 145644 and 54472).

Cluster 4: Sample 125492 belonged to the fourth cluster with a melt temperature of 70.2ºC

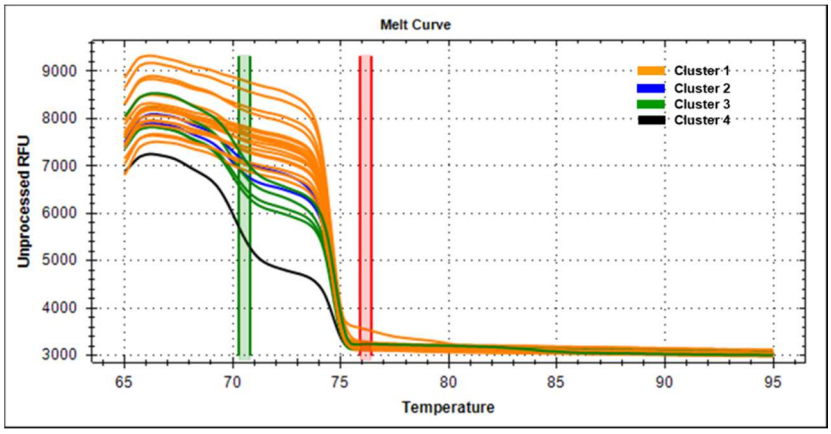

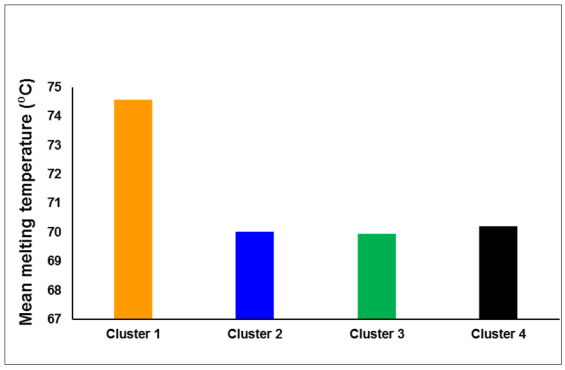

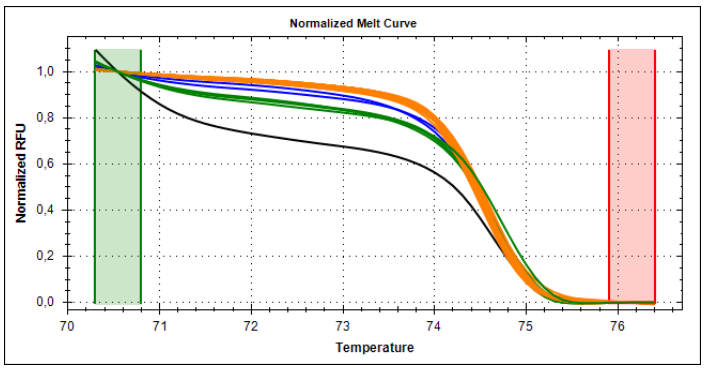

Figure 23: The BDNF melt curve profile generated by the HRM real-time PCR system and analysed using the Precision Melt Software. (A) The pre-melt (green vertical line) and the post-melt (red vertical line) fluorescent signals of all the 25 placenta samples; (B) The melt curve normalised to relative values 1 and 0; (C) the average melting temperature (T_m) for each cluster.

Sanger sequencing: Sanger sequencing was carried out to identify methylation of CpG nucleotides, if any, and the positions at which they have got methylated. Two samples representative of each cluster (Cluster 1: Sample 7032 and C151676; Cluster 2: 105086 and C12939; Cluster 3: 145644 and 54472; Cluster 4: 125492) was sent for Sanger sequencing (Eurofins Genomics). BDNF forward primer was used for sequencing.

The DNA sequences were imported and aligned in the alignment editor of GeneStudio software. The aligned sequences were compared with the amplified region of the BDNF gene as given in Figure 23. Figure 24 shows the 5' region of the aligned Sanger sequences. The CREB region of BDNF is highlighted in blue square box. In the CREB region, cytosine residues (considered to be methylated) could be observed only for sample C12939 (Cluster 2). A few cytosine nucleotides were present at the beginning of the 5' end of samples 145644 and 54472 (Cluster 3) but were lost due to trimming of the starting nucleotides. Sample 125492 (Cluster 4) showed the presence of cytosine residues in the chromatogram (marked by single letter code 'M'). Samples 7032 and C151676 (Cluster 1) did not show any changes.

To sum up, it is possible that low levels of methylation occurred at regions other than CpGs (non-CpG sites) in some samples and this resulted in sample clustering in HRM. Use of a standard curve in future experiments could help to determine the degree of methylation. Moreover, single nucleotide polymorphisms and heterogeneous genotypes could also result in the formation of clusters in HRM. Heterogenous alleles do not exhibit the same T_m as methylated cytosines and could have lower T_m.

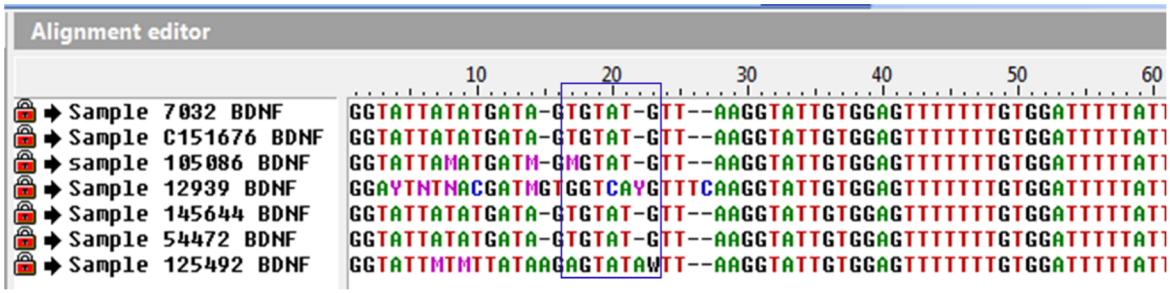

Figure 24 shows Sanger DNA sequences of BDNF PCR product. The CREB region is highlighted in blue. The cytosine nucleotides are observed at CREB region of sample 12939. Samples 7032 and C151676 did not show any nucleotide changes (Single letter code M= A or C; Y= C or T; N= A or C or G or T).

5.7.4 RNA quality assessment

For the first set of samples, RNA concentration ranged between 18-26 ng/ µl. The agarose gel image (Figure 25) shows the RNA quality from INMA placentas. The samples were loaded in the following order (Sample No 1: 7032, Sample No 2: 100208, Sample No 3: 327759, Sample No 4: 107660, Sample No 5: 49402 and Sample No 6: 146260) Smeared RNA bands were observed with the absence of 2:1 ratio for 28S and 18S RNA indicating low RNA quality due to degradation.

The figure shows 1% agarose gel with smeared RNA indicating low RNA quality. Increased intensity of 5S rRNA bands could be visualised indicating degradation. The typical 2:1 ratio of 28S and 18S rRNA could not be observed.

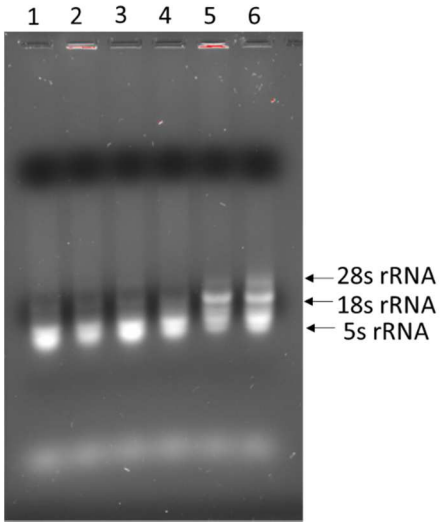

Figure 25: RNA quality from INMA placentas

For the second set of samples (Sample Nos. 122741, 105086, 37716, 39897, 27759, 107660, 7032, 100208, 146266) that were analysed by using Bioanalyser, the following peak patterns were observed. The RNA integrity value (RIN value) which allows to assess RNA integrity was found to be below 2.6 for all the INMA placenta samples.

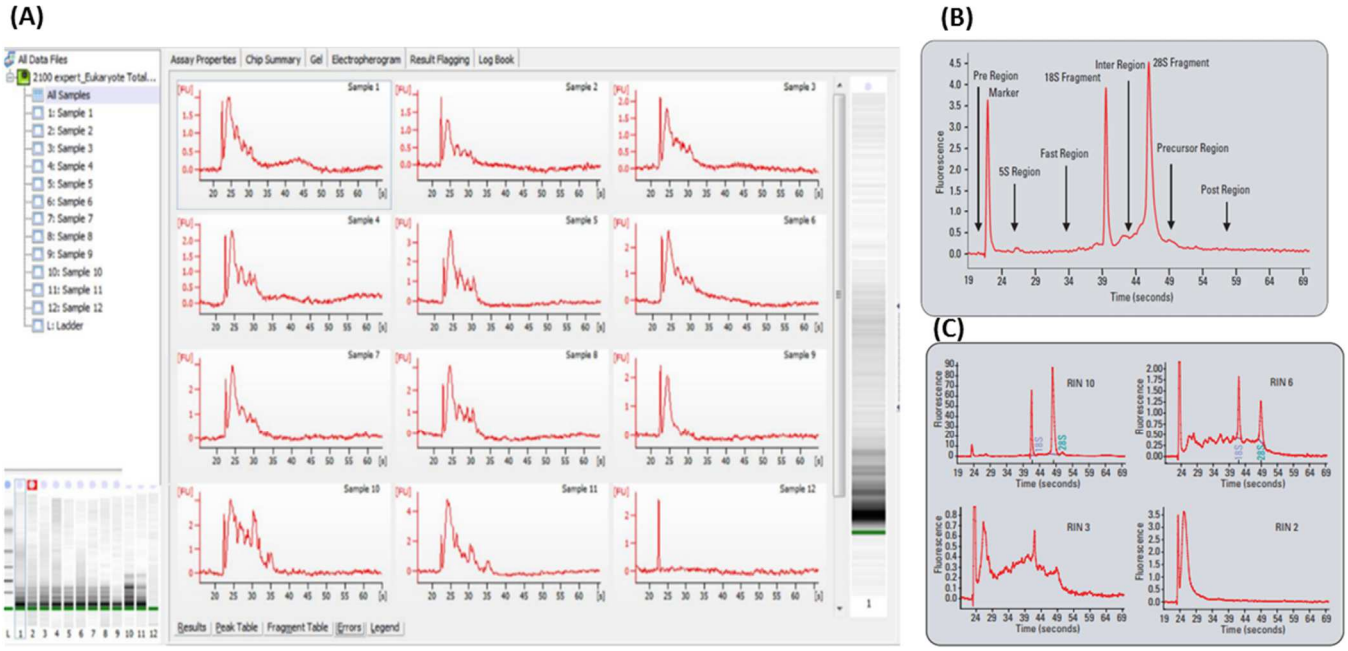

Figure 26: (A) shows Bioanalyser analyses report for seven INMA samples as per the order given in the methodology. Absence of 28S and 18S RNA can be observed with an increased peak at the marker and 5S region indicating degradation. (B) The image shows the typical peaks that corresponds to good quality RNA (C) the RNA integrity values ranging from 10 for good quality samples, and 2 for degraded samples (source of images 1B and 1C: https://www.agilent.com/cs/library/applications/5989-1165EN.pdf)

6 Conclusions

A lot of information has been produced and collected so far, highlighting the technical and scientific potential of the teams that have participated in this task. The 25 placental samples have been well characterised regarding exposure to metals, PFAS, steroid hormones, as well as for some specific biomarkers, metabolomics, epigenetic markers, telomere length and DNA damage. Additionally, an important collective effort has been made in order to characterise the combined estrogenic, anti-androgenic, anti-thyroid and aryl hydrocarbon biological activities elicited by environmental lipophilic chemical mixtures isolated from the placentas. A future ongoing step will be the study of possible relationships and correlations among the assessments conducted, in order to deepen the knowledge regarding the potential effects of complex chemical mixtures, and the potential use of effect biomarkers in HBM studies.

6.1 PFAS measurements in placental homogenates (INRA)

A total of 5 subtypes of PFAS (PFHxS, PFOS, PFOA, PFNA and PFDA) were detected in all the 25 placental alpha fractions extracts from the Spanish INMA birth cohort. Detection rates observed for PFHxS and PFDA were 96 and 68% respectively. Detection rates for other monitored PFAS markers ranged between 0 and 36%.

6.2 Metal profile in placental homogenates (INSERM)

Metal analyses were performed on the 25 placenta samples from the Spanish INMA birth cohort. Zn, Cu, Se, Pb, Hg, Cd, Cs, Na, Ca, K, Fe, Mg, Sr and Co were detected in all placenta samples. Ba, Ag and Al were detected with a 50% frequency in placenta samples while Ce, Bi, Mo, Sb, La, As, Mn and Cr were detected in 20 to 42% of placenta samples. Finally, Ti, Th, Tl and Ni were detected in less than 10% of placenta samples. Be, V, U, Li, Ru, Nd, Gd and Lu are not detected in all placenta samples.

6.3 Hormonal profile in placental homogenates (INRA)

A total of 24 hormones (free and total profile) were detected in all placental homogenates. As a next step, further correlations between hormonal profiles and the rest of exposure and effect biomarkers will be studied.

6.4 Untargeted metabolomics (INSERM-INRA-CEA)

This preliminary data on placenta homogenates using untargeted analyses have allowed identifying two metabolomics clusters. Compounds discriminating between clusters 1 and 2 include some prostaglandins (E2 and D2). Further work is required to identify significant differences between these two clusters. Moreover, more information on the samples is needed to draw any conclusions from these observations.

6.5 Anti-androgenic activity of placental alpha fractions (DTU)

The AR assay showed that all the tested placenta extract samples had varying AR antagonistic activity. However, the current data cannot give any information of the specific substances responsible for the antagonistic activity. To get information of what substances could potentially be contributing to the AR antagonistic effect of the extract, a focused chemical analysis must be run on the extract samples (looking for known biophores of AR antagonistic compounds).

Moreover, six out of the 24 extracts (1, 7, 8, 9, 12 and 16) showed compromised cell viability of more than 20% at the lowest dilution of 60 times.

6.6 Urinary measurement for 8-OHdG (MU)

MU successfully developed a methodology to assess 8OHdG in urine samples. Further results and analyses are necessary to test the relationship between 8OHdG levels and oxidative stress found in urine and placenta samples.

6.7 Epigenetics Biomarkers (INSERM)

6.7.1 Histone H2AX Phosphorylation (Gamma-H2AX)

Gamma-H2AX is a very sensitive and reliable marker of early DNA damage. Western blot analyses showed varied expression of gamma-H2AX in the placenta samples. Based on gamma H2AX levels, a biomarker of DNA damage response, we clustered 25 placenta samples into four groups. More information on the samples may be needed to draw conclusions from these observations.

6.7.2 Trimethylation of histone 3 at lysine 4 (H3K4me3)

We studied the H3K4me3 levels at various nuclear receptors and other target genes in 12 placenta samples. H3K4me3 is a mark that is primarily associated with transcription start site and is involved in gene transcription. We studied H3K4me3 enrichment at the promoters of some nuclear receptors, BDNF and gamma H2AX. Globally, the analysis of H3K4me3 occupancy at the promoters of nuclear receptors in low and high gamma-H2AX groups showed an increase in H3K4me3 occupancy at the promoter of progesterone receptor (PGR) indicating possible transcription activity at the promoter of PGR. Larger sample numbers may be necessary to confirm the results with statistical power and precision.

6.7.3 DNA methylation of BDNF

High-resolution melt analysis of the BS-converted placental DNA showed 4 clusters indicating changes in nucleotides although the differences were very subtle. HRM at the promoter of BDNF IV followed by Sanger sequencing showed the presence of cytosine residues in the CREB region of two samples that belonged to high gamma H2AX cluster. Further studies are required to confirm whether these nucleotide changes result in any phenotype alterations. This proof of concept study provides evidence for changes in the nucleotides in some samples following BDNF amplification and the ability of HRM to detect these minute changes resulting in the formation of clusters. A standard methylation curve with known levels of methylation will help identify the methylation levels in each cluster which we shall carry out in the future studies.

6.7.4 RNA quality assessment

Both agarose gel and Bioanalyser results confirmed total degradation of RNA in the placenta samples.

7 Future Steps

- The comparison of these data with other similar existing/published data, as well as their relation with other markers of effect variables is now on-going. Thus, possible relationships and correlations among the combined biological activities characterised in response to isolated mixtures of lipophilic chemicals and the rest of effect markers characterised will be studied. Additionally, the relationship between biomarkers of exposure (i.e, metals and PFAS) in relation to biomarkers of effect tested (i.e, oxidative stress, steroid hormones and epigenetic markers) will also be explored.
- CEA is currently acquiring the data of non-targeted LC-HRMS profiling of polar and non-polar fractions. The mass spectrometry data acquisition is being performed with very high-resolution Orbitrap Fusion TM Tribrid TM mass spectrometer using electrospray ionisation in positive and negative mode. Separation will be performed using high performance liquid chromatography on a Dionex Ultimate 3000 equipped either with a SeQuant® Zic-pHILIC® column (for the separation of the more polar compounds) or a Hypersil GoldTM C18 column.
- INRA plans (end 2018-beginning 2019) to look for halogenated marker of exposure possibly present in these extracts, through the use of a dedicated bioinformatics tool developed in the frame of this project (HaloSseeker software). Regarding the polar extract, C_{18} reverse phase chromatography does not appear as the optimal conditions to analyse it because main of compounds are quickly eluted. An alternative hydrophilic interaction chromatography (HILIC) is then envisaged (first trimester 2019) to reach a better separation efficiency for these polar compounds.
- CEA is planning to annotate with its in-house reference mass spectrum library the different LC-HRMS profiles generated (end 2018 – beginning 2019). It is also planned to transfer the obtained LC-HRMS raw data to INRA and INSERM (end 2018) for more specific data annotation (e.g. halogenated compounds or steroids annotation). Depending on the preliminary results and if relevant unknown (non-annotated) markers are detected, structural elucidation will be investigated by additional LC-HRMS/MS experiments.
- AU will work on a specific method for placenta and serum fractionation and isolation of mixtures of PFAS metabolites, that will be tested for ER transactivity. See the table below:

Table13: Schedule followed by AU to conduct the on-going isolation of PFAS.

Week	Procedure plan
47 19.-23. November: *Setting trails*	**Extraction of PFAS from 3-4 placenta samples** Test of homogenisation procedure (protocol based on ref 1 - 6) Test of placenta amount (protocol based on ref 1 - 6) SPE-HPLC-WAX procedure
48 26.-30. November: *Setting trails*	**Test of PFAS placenta extract induced estrogen receptor transactivity in cell culture** Test of extract concentrations Test of cell viability to placenta extracts
Data evaluation and Revision of the protocols	
49 3.-7. December	**Extraction of PFAS from 21-22 placenta samples** SPE-HPLC-WAX procedure
50 10.-14. December	**Measuring the PFAS placenta extracts induced estrogen receptor transactivity** 21-22 PFAS placenta extracts with and without co-exposure by estrogen (E2) to evaluate the possible competition between PFAS and endogenous estradiol hormones
51 17.-21. December	**Finalising the report** Final data analyses and writing the report

8 References

Aquino, E.M., Benton, M.C., Haupt, L.M., Sutherland, H.G., Griffiths, L.R., Lea. R.A., 2018. Current Understanding of DNA Methylation and Age-related Disease. OBM Genetics; 2:1-17 htpps://doi.org/10.21926/obm.genet.1802016

Arrebola, J.P., Molina-Molina, J.M., Fernández, M.F., Sáenz, J.M., Amaya, E., Indiveri, P., Hill, E.M., Scholze, M., Orton, F., Kortenkamp, A., Olea, N., 2015. A novel biomarker for anti-androgenic activity in placenta reveals risks of urogenital malformations. Reproduction 149, 605–13. https://doi.org/10.1530/REP-14-0525

ATSDR, undefined, 2009. Toxicological Profile for Perfluoroalkyls.

Autry, A.E., Monteggia, L.M., 2012. Brain-derived neurotrophic factor and neuropsychiatric disorders. Pharmacol Rev; 64: 238-258. htpps://doi.org/:10.1124/pr.111.005108.

Ballesteros, V., Costa, O., Iñiguez, C., Fletcher, T., Ballester, F., Lopez-Espinosa, M.J., 2017. Exposure to perfluoroalkyl substances and thyroid function in pregnant women and children: A systematic review of epidemiologic studies. Environ Int. 99:15-28. htpps://doi.org/10.1016/j.envint.2016.10.015.

Bathina S., Das U.N., 2015. Brain-derived neurotrophic factor and its clinical implications. Arch Med Sci; 11: 1164-1178. htpps://doi.org/10.5114/aoms.2015.56342

Bjerregaard-Olesen, C., Ghisari, M., Bonefeld-Jørgensen, E.C., 2016. Activation of the estrogen receptor by human serum extracts containing mixtures of perfluorinated alkyl acids from pregnant women. Environ. Res. 151, 71–79. https://doi.org/10.1016/j.envres.2016.07.001

Blake, B.E., Pinney, S.M., Hines, E.P., Fenton, S.E., Ferguson, K.K., 2018. Associations between longitudinal serum perfluoroalkyl substance (PFAS) levels and measures of thyroid hormone, kidney function, and body mass index in the Fernald Community Cohort. Environ. Pollut. 242, 894–904. https://doi.org/10.1016/j.envpol.2018.07.042

Bonefeld-Jorgensen, E.C., Long, M., Bossi, R., Ayotte, P., Asmund, G., Krüger, T., Ghisari, M., Mulvad, G., Kern, P., Nzulumiki, P., Dewailly, E., 2011. Perfluorinated compounds are related to breast cancer risk in Greenlandic Inuit: a case control study. Environ. Health 10, 88. https://doi.org/10.1186/1476-069X-10-88

Bonisch C., Hake S.B., 2012. Histone H2A variants in nucleosomes and chromatin: more or less stable? Nucleic Acids Res; 40: 10719-10741. htpps://doi.org/10.1093/nar/gks865.

Courant, F., Aksglaede, L., Antignac, J.P., Monteau, F., Sorensen, K., Andersson, A.M., Skakkebaek, N.E., Juul, A., Bizec, B.L., 2010. Assessment of circulating sex steroid levels in prepubertal and pubertal boys and girls by a novel ultrasensitive gas chromatography-tandem mass spectrometry method. J Clin Endocrinol Metab. 95(1):82-92. https://doi.org/10.1210/jc.2009-1140.

Deaton, A.M., Bird, A., 2011. CpG islands and the regulation of transcription. Genes Dev 25, 1010-1022. htpps://doi.org/10.1101/gad.2037511.

DeCaprio, A.P., 1997. Biomarkers: Coming of Age for Environmental Health and Risk Assessment. Environ. Sci. Technol. 31, 1837–1848. https://doi.org/10.1021/es960920a

Deng, P., Anderson, J.D., Yu, A.S., Annett, G., Fink, K.D., Nolta, J.A., 2016. Engineered BDNF producing cells as a potential treatment for neurologic disease. Expert Opin Biol Ther; 16:1025-1033. htpps://doi.org/10.1080/14712598.2016.1183641

Dong, X., Weng, Z., 2013. The correlation between histone modifications and gene expression. Epigenomics; 5: 113-116. htpps://doi.org/10.2217/epi.13.13.

Esposito, F., Nardone, A., Fasano, E., Scognamiglio, G., Esposito, D., Agrelli, D., Ottaiano, L., Fagnano, M.,

Adamo, P., Beccaloni, E., Vanni, F., Cirillo, T., 2018. A systematic risk characterization related to the dietary exposure of the population to potentially toxic elements through the ingestion of fruit and vegetables from a potentially contaminated area. A case study: The issue of the "Land of Fires" area in Campania region, Italy. Environ. Pollut. 243, 1781–1790. https://doi.org/10.1016/j.envpol.2018.09.058

Feinshtein, V., Ben-Zvi, Z., Sheiner, E., Amash, A., Sheizaf, B., Holcberg, G., 2010. Progesterone levels in cesarean and normal delivered term placentas. Arch Gynecol Obstet 281, 387-392. htpps://doi.org/ 10.1007/s00404-009-1125-x.

Fernandez, M.F., Olmos, B., Granada, A., López-Espinosa, M.J., Molina-Molina, J.M., Fernandez, J.M., Cruz, M., Olea-Serrano, F., Olea, N., 2007. Human exposure to endocrine-disrupting chemicals and prenatal risk factors for cryptorchidism and hypospadias: a nested case-control study. Environ Health Perspect. 115 Suppl 1:8-14. https://doi.org/10.1289/ehp.9351.

Fisher, M., Arbuckle, T.E., Wade, M., Haines, D.A., 2013. Do perfluoroalkyl substances affect metabolic function and plasma lipids?—Analysis of the 2007–2009, Canadian Health Measures Survey (CHMS) Cycle 1. Environ. Res. 121, 95–103. https://doi.org/10.1016/J.ENVRES.2012.11.006

Fu, J., Gao, Y., Cui, L., Wang, T., Liang, Y., Qu, G., Yuan, B., Wang, Y., Zhang, A., Jiang, G., 2016. Occurrence, temporal trends, and half-lives of perfluoroalkyl acids (PFAAs) in occupational workers in China. Sci. Rep. 6, 38039. https://doi.org/10.1038/srep38039

Guenther, M.G., Levine, S.S., Boyer, L.A., Jaenisch, R., Young, R.A., 2007. A chromatin landmark and transcription initiation at most promoters in human cells. Cell; 130: 77-88. htpps://doi.org/10.1016/j.cell.2007.05.042.

Ji, J., Zhang, Y., Redon, C.E., Reinhold, W.C., Chen, A.P., Fogli L.K., Holbeck S.L., Parchment R.E., Hollingshead M., Tomaszewski J.E., Dudon Q., Pommier Y., Doroshow J.H., Bonner W.M., 2017. Phosphorylated fraction of H2AX as a measurement for DNA damage in cancer cells and potential applications of a novel assay. PLoS One; 12: e0171582. htpps://doi.org/10.1371/journal.pone.0171582.

Karlic, R., Chung, H.R., Lasserre, J., Vlahovicek, K., Vingron, M., 2010. Histone modification levels are predictive for gene expression. Proc Natl Acad Sci USA; 107:2926-2931. htpps://doi.org/ 10.1073/pnas.0909344107.

Karve, TM., Cheema, A.K., 2011. Small changes huge impact: the role of protein posttranslational modifications in cellular homeostasis and disease. J Amino Acids; 2011: 207691. htpps://doi.org/10.4061/2011/207691.

Kinner, A., Wu, W., Staudt, C., Iliakis, G., 2008. Gamma-H2AX in recognition and signaling of DNA double-strand breaks in the context of chromatin. Nucleic Acids Res; 3:, 5678-5694. htpps://doi.org/ 10.1093/nar/gkn550.

Kortenkamp, A., 2014. Low dose mixture effects of endocrine disrupters and their implications for regulatory thresholds in chemical risk assessment. Curr. Opin. Pharmacol. 19, 105–11. https://doi.org/10.1016/j.coph.2014.08.006

Kouzarides, T., 2007. Chromatin modifications and their function. Cell; 128: 693-705. https://doi.org/10.1016/j.cell.2007.02.005

Kundakovic, M., Gudsnuk, K., Herbstman, J.B., Tang, D., Perera, F.P., Champagne, F.A., 2015. DNA methylation of BDNF as a biomarker of early-life adversity. Proc Natl Acad Sci USA; 112: 6807-6813. htpps://doi.org/ 10.1073/pnas.1408355111.

Lin, C.-Y., Chen, P.-C., Lin, Y.-C., Lin, L.-Y., 2009. Association among serum perfluoroalkyl chemicals, glucose homeostasis, and metabolic syndrome in adolescents and adults. Diabetes Care 32, 702–7. https://doi.org/10.2337/dc08-1816

Lindstrom, A.B., Strynar, M.J., Libelo, E.L., 2011. Polyfluorinated Compounds: Past, Present, and Future. Environ. Sci. Technol. 45, 7954–7961. https://doi.org/10.1021/es2011622

Lu, B., Nagappan, G., Lu Y., 2014. BDNF and synaptic plasticity, cognitive function, and dysfunction. Handb Exp Pharmacol; 220: 223-250.

Marzluff, W.F., Gongidi, P., Woods, K.R., Jin, J., Maltais, L.J., 2002. The human and mouse replication-dependent histone genes. Genomics; 80: 487-498. https://doi.org/10.1006/geno.2002.6850

Pastor-Barriuso, R., Fernández, M.F., Castaño-Vinyals, G., Whelan, D., Pérez-Gómez, B., Llorca, J., Villanueva, C.M., Guevara, M., Molina-Molina, J.-M., Artacho-Cordón, F., Barriuso-Lapresa, L., Tusquets, I., Dierssen-Sotos, T., Aragonés, N., Olea, N., Kogevinas, M., Pollán, M., 2016. Total Effective Xenoestrogen Burden in Serum Samples and Risk for Breast Cancer in a Population-Based Multicase-Control Study in Spain. Environ. Health Perspect. 124, 1575–1582. https://doi.org/10.1289/EHP157

Patel, C.J., Yang, T., Hu, Z., Wen, Q., Sung, J., El-Sayed, Y.Y., Cohen, H., Gould, J., Stevenson, D.K., Shaw, G.M., Ling, X.B., Butte, A.J., 2014. Investigation of maternal environmental exposures in association with self-reported preterm birth. Reprod. Toxicol. 45, 1–7. https://doi.org/10.1016/j.reprotox.2013.12.005

Rehman, K., Fatima, F., Waheed, I., Akash, M.S.H., 2018. Prevalence of exposure of heavy metals and their impact on health consequences. J. Cell. Biochem. 119, 157–184. https://doi.org/10.1002/jcb.26234

Robinson, D.P., Klein, S.L., 2012. Pregnancy and pregnancy-associated hormones alter immune responses and disease pathogenesis. Horm Behav; 62 : 263-271. htpps://doi.org/10.1016/j.yhbeh.2012.02.023.

Rogakou, E.P., Boon, C., Redon, C., and Bonner, W.M., 1999. Megabase chromatin domains involved in DNA double-strand breaks in vivo. J Cell Biol; 146: 905-916.

Saxonov, S., Berg, P., Brutlag, D.L., 2006. A genome-wide analysis of CpG dinucleotides in the human genome distinguishes two distinct classes of promoters. Proc Natl Acad Sci USA; 103: 1412-1417. htpps://doi.org/10.1073/pnas.0510310103.

Sharma, A., Singh, K., Almasan, A., 2012. Histone H2AX phosphorylation: a marker for DNA damage. Methods Mol Biol; 920: 613-626. htpps://doi.org/ 10.1007/978-1-61779-998-3_40.

Shankar, A., Xiao, J., Ducatman, A., 2011. Perfluoroalkyl Chemicals and Chronic Kidney Disease in US Adults. Am. J. Epidemiol. 174, 893–900. https://doi.org/10.1093/aje/kwr171

Shilatifard, A., 2012. The COMPASS family of histone H3K4 methylases: mechanisms of regulation in development and disease pathogenesis. Annu Rev Biochem; 81: 65-95. htpps://doi.org/ 10.1146/annurev-biochem-051710-134100.

Silbergeld, E.K., Davis, D.L., 1994. Role of biomarkers in identifying and understanding environmentally induced disease. Clin. Chem. 40, 1363–1367.

Smagulova, F., Gregoretti, I.V., Brick, K., Khil, P., Camerini-Otero, R. D., Petukhova, G. V., 2011. Genome-wide analysis reveals novel molecular features of mouse recombination hotspots. Nature *472*, 375-378. htpps://doi.org/ 10.1038/nature09869.

Starkman, B.G., Sakharkar, A.J., Pandey, S.C., 2012. Epigenetics-beyond the genome in alcoholism. Alcohol Res *34*, 293-305.

Talbert, P., Henikoff, S., 2010. Histone variants--ancient wrap artists of the epigenome. Nat Rev Mol Cell Biol; 11: 264-275. htpps://doi.org/10.1016/B978-0-12-380866-0.60005-8.

Vilahur, N., Fernández, M.F., Bustamante, M., Ramos, R., Forns, J., Ballester, F., Murcia, M., Riaño, I., Ibarluzea, J., Olea, N., Sunyer, J., 2014. In utero exposure to mixtures of xenoestrogens and child

neuropsychological development. Environ. Res. 134, 98–104. https://doi.org/10.1016/j.envres.2014.07.002

Vilahur, N., Molina-Molina, J.M., Bustamante, M., Murcia, M., Arrebola, J.P., Ballester, F., Mendez, M.A., Garcia-Esteban, R., Guxens, M., Santa Marina, L., Tardón, A., Sunyer, J., Olea, N., Fernandez, M.F., 2013. Male specific association between xenoestrogen levels in placenta and birthweight. Environ. Int. 51, 174–81. https://doi.org/10.1016/j.envint.2012.10.004

Watkins, D.J., Josson, J., Elston, B., Bartell, S.M., Shin, H.-M., Vieira, V.M., Savitz, D.A., Fletcher, T., Wellenius, G.A., 2013. Exposure to Perfluoroalkyl Acids and Markers of Kidney Function among Children and Adolescents Living near a Chemical Plant. Environ. Health Perspect. 121, 625–630. https://doi.org/10.1289/ehp.1205838

Wozniak, G.G., Strahl, B.D., 2014. Hitting the 'mark': interpreting lysine methylation in the context of active transcription. Biochim Biophys Acta; 1839 : 1353-1361. htpps://doi.org/10.1016/j.bbagrm.2014.03.002.

Zhao, L., Chang, D. W., Gong, Y., Eng, C., Wu, X., 2017. Measurement of DNA damage in peripheral blood by the gamma-H2AX assay as predictor of colorectal cancer risk. DNA Repair (Amst) *53*, 24-30. htpps://doi.org/10.1016/j.dnarep.2017.03.001.

Zuccato, C., Cattaneo, E., 2009. Brain-derived neurotrophic factor in neurodegenerative diseases. Nat Rev Neurol; 5: 311-322. htpps://doi.org/10.1038/nrneurol.2009.54.